
5G
and
IoT
2015
Mobile Communications & Infrastructure
A SPECIAL SUPPLEMENT TO
Microwave Journal

Table of Contents

AUGMENTED REALITY: HOW IT WORKS

STEP 1
Download the free Layar app from the iTunes (iOS) or Google Play (Android) store.

STEP 2
Launch the app to view enhanced content on any page with the layar logo.

STEP 3
Frame the entire page in the screen and tap to experience enhancements (tap screen again for full screen view).

Look for the Layar logo on participating pages. AR pages may expire after 30 days.

Staff

Publisher: Carl Sheffres
Editor: Patrick Hindle
Technical Editor: Gary Lerude
Managing Editor: Jennifer DiMarco
Associate Technical Editor: Cliff Drubin
Multimedia Staff Editor: Leslie Nikou
Multimedia Staff Editor: Barbara Walsh
Consulting Editor: Harlan Howe, Jr.
Consulting Editor: Frank Bashore
Consulting Editor: Raymond Pengelly

Electronic Marketing Manager: Chris Stanfa
Client Services Manager: Kristen Anderson
Event Coordinator: Jacqueline Williams
Audience Development Manager: Carol Spach
Traffic Manager: Edward Kiessling
Director of Production & Distribution: Robert Bass
Art Director: Janice Levenson
Graphic Designer: Sachiko Stiglitz

EUROPE

International Editor: Richard Mumford
Office Manager: Nina Plesu

CORPORATE STAFF

CEO: William M. Bazzy
President: Ivar Bazzy
Vice President: Jared Bazzy

BPA WORLDWIDE

Scan page using layar app

COVER FEATURE
INVITED PAPER

Highly Integrated Silicon ASICs: a Disruptive Technology for AESAs

Ian Gresham, Rob McMorrow, David Corman and Nitin Jain
Anokiwave Inc., San Diego, Calif.

Active electronically scanned array (AESA) antennas have been employed for military phased array radar systems for over five decades. Their popularity has dramatically increased recently as advances in technology enable compact, low cost arrays for commercial applications.[1] As they are adopted for markets as disparate as weather radar, sense-and-avoid radar for commercial and private drones, global ground-satellite communication for Internet access as well as 5G infrastructure, they are poised to become even more prevalent.[2] Indeed, the use of phased array techniques to provide advanced antenna aperture capabilities is seen as fundamental to the rollout of 5G infrastructure.[3,4]

One of the driving technologies for this path to growing adoption is the increasing use of silicon-based (Si) technologies (SiGe BiCMOS and RF CMOS) to provide increased functional density and capability within a single die/package.[5] This article reviews some of the technical challenges of building high density planar phased arrays and suggests that solutions to these problems can be found by greatly increasing the level of integration in the IC solutions, thus enabling large-scale planar AESA arrays. By taking advantage of the integration capability of silicon, additional system level functionality such as on-chip diagnostics, built-in self-test (BIST) and built-in calibration (BICAL) can be utilized to give the end user far more visibility and control over the operation of the array. Examples of the performance features that can be embedded into highly integrated application specific integrated circuits (ASIC) used in silicon-based AESA arrays will be discussed.

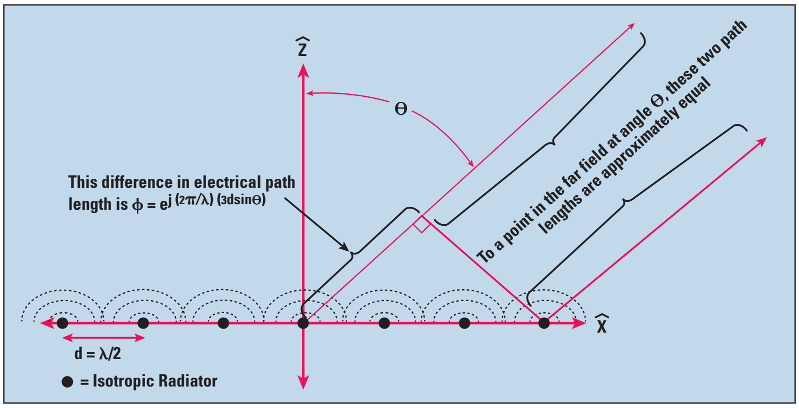

▲ *Fig. 1 Simplified one-dimensional planar array antenna consisting of a row of isotropic radiators. The far field antenna pattern is a composite of the excitations at each element.*

Figure 1 shows a simplified one-dimensional illustration of a phased array antenna, consisting of a row of isotropic radiators. The composite response of the antenna pattern in the far-field is a function of the amplitude and phase excitation at each element. Simplistically, the careful control of each amplitude and phase response determines the magnitude and scan angle of a single- or multi-beam antenna pattern. One of the constraints for a wide scan angle antenna pattern is the restriction that each of the antenna elements is spaced by no more than a free space half wavelength ($\lambda 0$) to

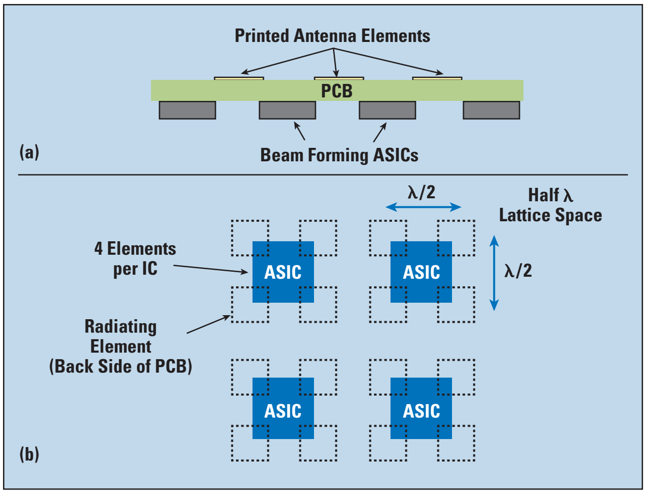

▲ *Fig. 2 Side (a) and plan (b) views, showing beam forming ASICs mounted on the backside of the planar antenna array.*

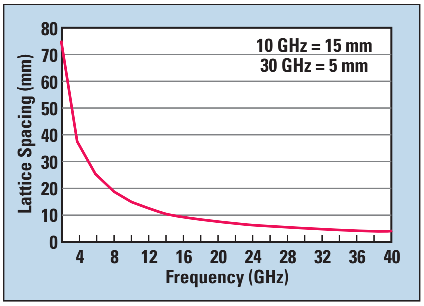

▲ *Fig. 3 Half wavelength lattice spacing vs. frequency.*

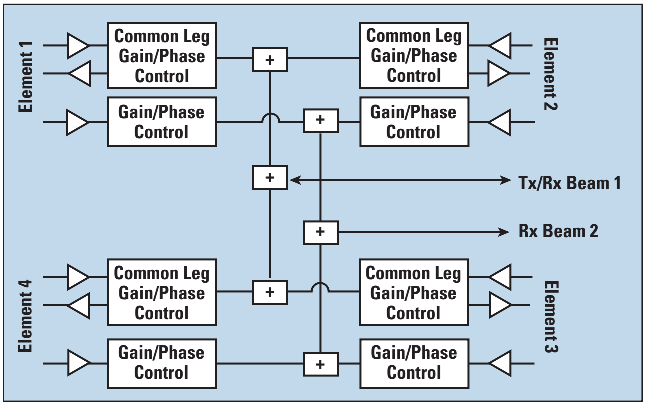

▲ *Fig. 4 Functional block diagram of the integrated TDD T/R chip.*

avoid the generation of grating lobes, where waves from each element are summed in phase producing beams in undesired directions.[6,7] Beamforming can be performed in either the analog or the digital domain (or both) with trade-offs in system performance for complexity, linearity and power dissipation.

Planar phased array antenna solutions are attractive in providing a compact, and potentially low-profile form, thus enabling their use in a broader range of applications.[2] The primary enabler for a planar-form solution is for the analog beamforming circuitry – transmit (Tx), receive (Rx) or transceiver (Xcvr) – to fit physically between the elements of the antenna lattice. ***Figure 2*** shows an illustration of how this may be realized, where the beamforming ASICs are surface mounted to a PCB with the antenna radiating surface on the opposite side. Note that in this highly idealized drawing, signal routing and heat sinks for thermal power management are not shown.

So far, so good. But the challenge of this approach can be appreciated by considering how the available physical dimensions rapidly shrink as a function of frequency. To a first order, the lattice spacing between antenna elements is constrained to a half wavelength to avoid the presence of grating lobes, which is plotted in ***Figure 3*** as a function of the operating frequency. (In reality, the maximum spacing is also a function of the maximum required scan angle). The physical constraints governing the available area for component integration falls dramatically from 37.5 mm at 4 GHz (S-Band) to 15 mm at 10 GHz (X-Band) and only 5 mm at 30 GHz (Ka-Band).

Unfortunately, discrete based solutions in commercially available surface mount device (SMD) packages can easily exceed these limitations, as their combined area and allowance for interconnects and support componentry occupy a large footprint. At X-Band and above, increased integration becomes the only way to make such a planar system a viable option. Solutions have become available in recent years that integrate single element beam formers with Tx/Rx functionality in a single package.[8] GaAs technologies that are commonly used for these functions due to their high electron mobility and associated performance metrics are expensive and limited in their integration capability. By comparison, high performance SiGe BiCMOS and RF CMOS have demonstrated the required performance at microwave and millimeter wave frequencies in multiple applications.[5] In addition, their ability to integrate dense functionality results in the potential for combining product solutions that can support multiple radiating elements within a single package. ***Figure 4*** is a functional block diagram of a single component that simultaneously supports dual polarization and four radiating elements.

HIGHLY INTEGRATED SOLUTION

This section reviews an example of how a highly integrated TDD (time-domain duplex) transmit-receive chip supporting four discrete antenna elements may be configured to meet the objective requirements of cost, size and functionality. It is packaged within a standard commercial QFN-style plastic package measuring 7 × 7 × 0.9 mm, and easily fits within the 15 mm lattice spacing at 10 GHz for X-Band applications. The IC consists of four distinct quadrants that can each be operated and controlled discretely, with the ability to simultaneously drive four antenna elements in transmit mode. In addition, there are eight independent receive ports – two per quadrant – that allow for dual polarization on each antenna element when operating in receive mode. Transmit and receive waveforms can be weighted independently with 12-bit complex vector modulators consisting of 6-bit phase control, where the least significant bit (LSB) is 5.625 degrees, and 6-bit amplitude control, providing 31.5 dB dynamic range and LSB of 0.5 dB.

Figure 4 shows this partitioning in more detail. Each quadrant consists of a Tx/Rx arm sharing a common path vector modulator (complex amplitude and phase) as well as a second receive-only arm which shadows the Tx/Rx function. Central to the quadrant based operation is a chip-core where the modulated received signals are coherently combined and feed a common RF port. The TDD based operation of the die allows the combiner network of the Tx/Rx arm to be used for coherent power splitting when operating in the transmit mode. Over 31 dB of dynamic range is therefore available in each discrete antenna element path through varying the discrete vector modulators. This dynamic range can be used for array taper or other gain control functions. The settings of each of the vector modulators, as well as the other functions on the chip, are controlled using a serial peripheral interface (SPI) for data transfer and control signal management.

Temperature compensation of the entire chip can be enabled through additional digital variable attenuators (DVA), allied with active gain stages in each of the common combiner ports to extend the controllable dynamic range of the IC to over 50 dB. This can be used in conjunction with an on-chip temperature sensor to account for temperature changes within the IC and also compensate other temperature sensitive components elsewhere in the system. Real-time, closed loop temperature compensation can be implemented by reading data from the IC temperature sensor, updating the appropriate settings and using available data for external components. Maximum system flexibility results from the gain control partitioning provided by the chip.

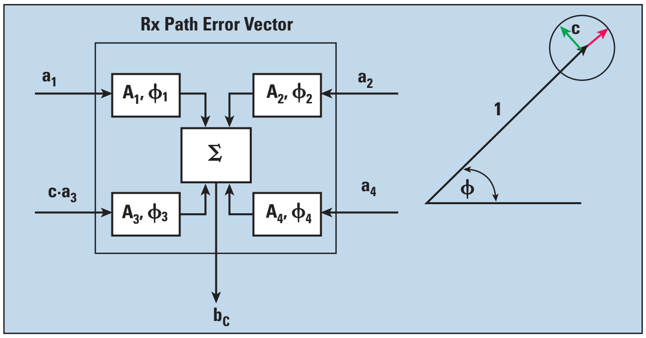

▲ *Fig. 5 Unwanted signal coupling degrades modulated waveform accuracy, inducing AM-AM and AM-PM errors.*

PHASE AND AMPLITUDE ACCURACY

Although an increase in the number of antenna elements that can be supported by a single component, by utilizing the benefits of the functional integration density of Si, has several advantages (i.e., reduced bill-of-materials, reduced inventory, smaller PCB integration form-factor), it is not an approach that can be followed with impunity. Other functional and performance considerations include the ease of routing low-loss and controlled impedance transitions between the various RF ports and the antenna elements, thermal dissipation paths, the number of external components, signal and supply path constraints and unwanted signal coupling.

Figure 5 shows how signal coupling and appropriate isolation between signal paths needs to be considered and the potential limitations they may impose on system performance. In this example, four discrete Rx paths – a_1, a_2, a_3, and a_4 – are input to a common beamformer IC and coherently combined with a summed output signal of bc. Ideally, each of the four signal paths would remain isolated up to the input of the summing network, and the complex beam weight (Ai, ϕi) applied to each signal would have zero associated amplitude and phase error. In reality, non-idealities in each of the vector modulators and other components in each signal path will impose some level of AM-AM, PM-AM and AM-PM distortion, resulting in an associated error in the signal vector. In theory, any of these corrupting influences are well known and modeled during the design phase; as long as they are maintained below the magnitude of ½ LSB, they should not degrade performance.

More difficult to deal with is coupling between signal paths that may be less predictable, arising from several sources including signal transmission lines between the antenna elements and the component RF ports, signal coupling within the package through the unwanted radiation of bondwire transitions, dielectric material loading of the package over-mold and parasitic and leakage path coupling through other on-chip networks that are more difficult to account for at high frequencies.[9] These may include such disparate paths as bias distribution networks, pad-rings and ESD domain coupling. Regardless of the source, the effect illustrated in Figure

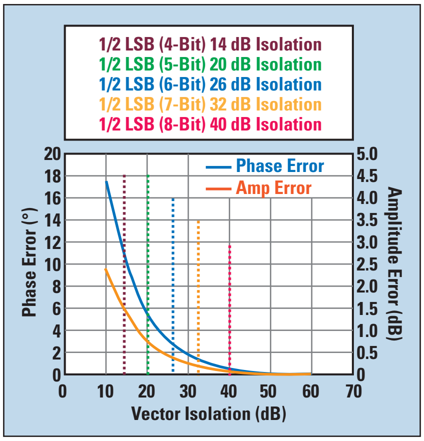

▲ *Fig. 6 Phase and amplitude error vs. coupled path isolation.*

5 produces the same result: distortion of the desired vector by a parasitic phasor that causes amplitude or phase distortion or both. In the simplest case, maximum amplitude error occurs when the coupled phasor is in phase with or exactly out of phase with the desired vector. Here, the magnitude of the error vector is

$$\Delta A_{error}(dB) = 20\log_{10}\left(1 \pm |c|\right) \qquad (1)$$

Similarly, the maximum phase error occurs when the coupled phasor is orthogonal to the phase of the desired vector, resulting in a maximum phase error of

$$\Delta\varphi_{error}(deg) = \tan^{-1}|c| \qquad (2)$$

The magnitude of the total amplitude and phase error of the desired vector needs to be maintained below ½ LSB, leading to a relationship between the number of available bits of amplitude and phase resolution and the allowable level of coupling between signal paths. ***Figure 6*** shows how this relationship varies for several combinations of vector modulator resolution. For example, to maintain the required accuracy for 6-bit amplitude and phase control, the magnitude of the worst case error vector needs to be less than 26 dB when normalized to a vector magnitude of 1. This figure, though, does not account for the effect of channel gain on the magnitude of the coupled signal. ***Figure 7*** shows how the level of coherent gain imposes more stringent requirements on the allowable coupling and drives increased channel-channel isolation. As the desired channel gain increases, the required coupling must decrease

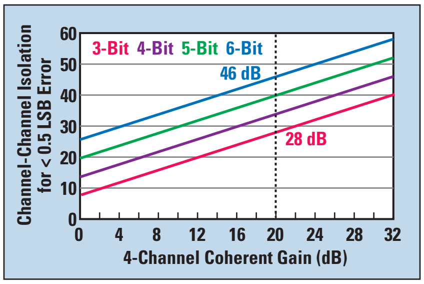

▲ *Fig. 7 Required minimum channel-channel isolation increases with coherent gain.*

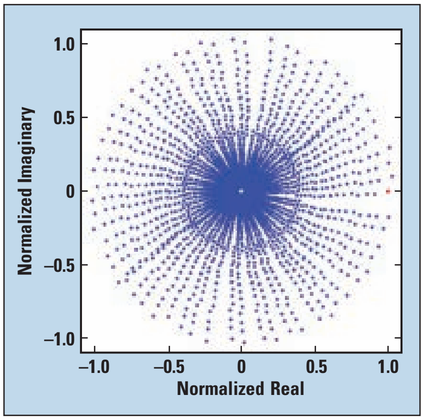

▲ *Fig. 10 Measured 12-bit vector modulator (6-bit amplitude and 6-bit phase) state map at 9.4 GHz.*

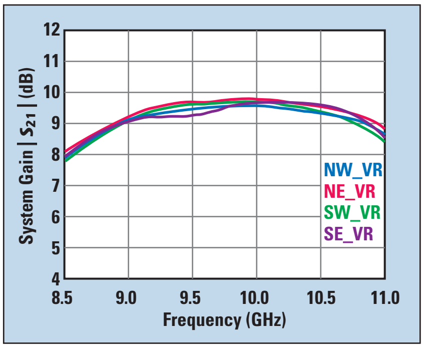

▲ *Fig. 8 Measured coherent receiver gain, showing < 1 dB imbalance across four channels.*

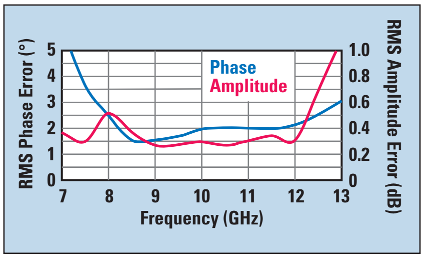

▲ *Fig. 11 Measured RMS amplitude and phase error across X-Band.*

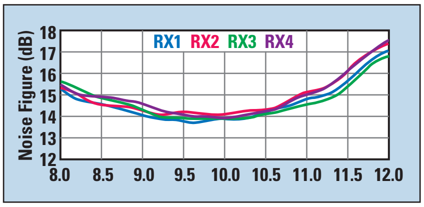

▲ *Fig. 9 Measured receiver noise figure. The four channels are assumed to be driven by non-coherent noise sources.*

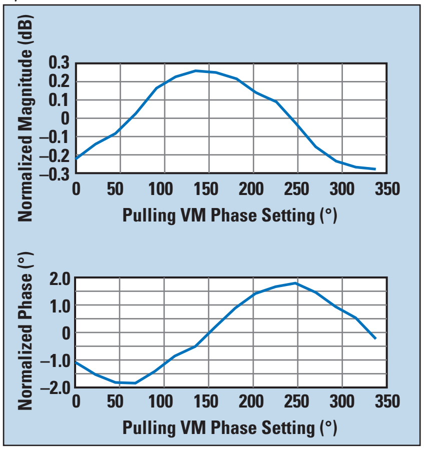

▲ *Fig. 12 Signal magnitude and phase error from unwanted signal coupling to adjacent ports.*

dB for dB to keep the same ½ LSB error. For example, if the channel gain is 20 dB and the vector modulator provides 6-bit complex modulation, the absolute isolation required becomes 26 dB + 20 dB or 46 dB.

ACTUAL PERFORMANCE METRICS

This section presents measured data for a commercially available 4-element beam former IC, to indicate the available performance for a highly integrated, multi-element solution. ***Figure 8*** shows the measured coherent receiver gain, which is defined as the combined (superimposed) signal gain between each of the four receiver ports and the output of the coherent combiner. The vector modulator for each signal path is set to a common complex beam weight for this measurement, resulting in a coherent gain that is approximately 7 dB across the band. The amplitude imbalance between the ports is < 1 dB, including mismatch. Noise figure (NF) versus frequency is shown in ***Figure 9***. This has been adjusted to reflect the NF seen when each port is driven from non-coherent noise sources. The NF at the center of the band is 14 dB. If only a single channel were measured, the resulting NF would be 4.1 dB higher. The input 1 dB compression point for the receiver is approximately -2 dBm at the center of the band. This is measured on a single channel.

The performance of the vector modulator is shown in ***Figure 10***. All 12 bits of amplitude and phase states (4,096 states) were measured and graphed on a polar plot. The concentric circles and linear spokes of the figure are indicative of the low PM-AM and AM-PM distortion of the vector modulator. ***Figure 11*** shows the explicit RMS phase and amplitude error across the band. The amplitude error is less than 0.5 dB, while the phase error is less than 3 degrees, or about 2/3 LSB. The channel-channel isolation can be inferred from a combination of measured S-parameters and beam rotation. A signal coupled to the common output port and superimposed upon the desired signal vector will cause AM-AM and AM-PM errors in the signal vector, as previously described. By measuring the signal path from any Rx input to the common output beam former port and adjusting the beam weight settings of the non-signal path vector modulators, the magnitude of the signal coupling into the main signal path can be estimated, as shown figuratively in Figure 5. The measured error in the phase response is approximately ±1.5 degrees as shown in ***Figure 12***, corresponding to a port-port isolation of approximately -38 dB, accounting for the coherent receiver gain.

ADVANCED FEATURES WITH INTEGRATION

The core technology enabler of dense functional integration is the ability to integrate multiple controllable circuit blocks within a single die using Si-based processes and control the operation using the SPI ports. It is then only a small additional step to use the access to the die provided by the SPI to embed supplementary functions and controls that can be controlled digitally by the customer to increase operational flexibility. In this example, a proprietary 5-wire, 50 MHz SPI has been used. This has been designed to minimize coupling between digital and RF signals. With the proprietary SPI bus, multiple ICs in a row or column or any other subset of an array can be daisy chained and driven by a single bus and latched in tandem.

In addition to the ability to write vectors to multiple registers, the SPI also allows read-back from functional blocks on the IC. This capability gives the array system integrator insight into real-time operation through the addition of on-chip telemetry. Each transmit arm includes an on-chip


32°C

power detector that samples the output signal with 5-bit resolution and provides the power measurement as a digital word to the SPI. In addition, the time at which the transmit power is measured can be determined by the user. This accommodates radar systems with varying pulse widths and also provides information on transmit pulse droop, if the measurement interval is varied pulse to pulse. ***Figure 13*** shows the detector output vs. power level and frequency. Similarly, on-chip temperature sensing provides real-time information and insight into the reliability of the IC.

Separate pins are provided to enable either transmit or receive mode, providing the flexibility to select the desired set-up time between activating transmit or receive DC power and when the RF waveform is applied. To minimize power dissipation, all transmit functions are powered down when the IC is in receive mode and vice-versa during transmit. The DC power consumption is 1.8 W in transmit, 1.7 W in receive if both receive beams (4-elements, dual polarization) are active and 1.3 W in receive if only one receive beam (4-elements, single polarization) is active. The chip is biased with a 1.8 V supply.

Another feature is the ability to set the chip in a calibration mode, where only one quadrant at a time is enabled. Separate pins are provided to communicate with an external front-end chip so that a complete channel-by-channel calibration can be performed. A further programming feature is the delay time between data latch and beam weight adjustment. The simultaneous change to all of the transmitters in a large array can create spurious lobes and system level problems. Dithering the time between latch and change for each IC can avoid this.

Lastly, programming the vector modulator for a single IC only takes 4.5 µs at 50 MHz. If a large number of ICs are daisy-chained for row-column addressing operations, the entire process can take substantially longer. One solution to this is to allow fast beam steering (FBS) by incorporating a programmable register stack with each vector modulator that can be pre-programmed with 12 bits of phase and amplitude information. Each vector modulator has a stack of eight registers that can be pre-loaded

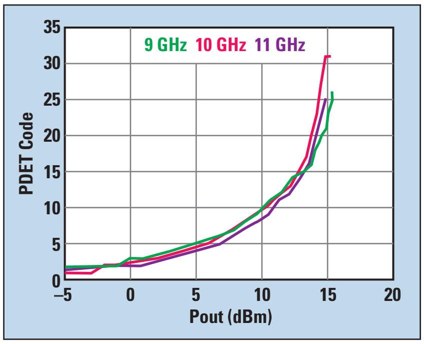

▲ *Fig. 13 Transmit path output power code vs. input power at 9, 10 and 11 GHz.*

using the SPI bus and then directly addressed via a 3-bit direct addressing parallel interface, eliminating the wait for a serial load via the SPI bus. This means that the beams can be switched in as fast as 50 ns. These two modes, programming on the fly and fast beam steering, provide flexibility for any radar application.

CONCLUSION

Planar AESAs require increased compaction of circuit functionality to maintain the required form factors at high frequencies. This is driven by the minimum lattice spacing requirements of antenna elements, to avoid the introduction of grating lobes in the radiation patterns of the antenna. One of the consequences of increased functional density is reducing the number of required components and reducing the cost for the entire bill-of-materials. A proven method for achieving this compaction is realizing the circuitry in a highly integrated Si IC. Additional benefits of this technology are the ability to integrate control and tuning elements to trim the optimal performance of the IC, using a serial interface, and providing telemetry for system monitoring, such as temperature and output power. Reducing the physical dimensions requires careful design to avoid limiting the accuracy of the available beam weight resolution through unwanted signal coupling paths; however, this has been shown to be possible. Other performance metrics possible with a 12-port IC supporting dual-polarization Tx/Rx receive functionality for a 4-element antenna solution have also been presented. ■

ACKNOWLEDGMENT

The authors thank the entire staff of Anokiwave for their ideas, enthusiasm and contributions to this work.

References

1. E. Brookner, “Phased-array Radars: Past, Astounding Breakthroughs and Future Trends,” *Microwave Journal*, January 2008.
2. G. Fields, “Phased-array Radar at The Intersection of Military and Commercial Innovation,” *Microwave Journal*, January 2014.
3. T. Rappaport et al., “Millimeter Wave Wirelesss Communications,” Prentice-Hall, 2015.
4. “IBM and Ericsson Collaborate on 5G Antenna Designs,” Ericsson press release, November 24, 2014.
5. G. Rebeiz et al., “Millimeter-Wave Large-Scale Phased-Arrays for 5G Systems,” IEEE MTT-S International Microwave Symposium, 2015.
6. R. C. Hansen, “Phased Array Antennas,” John Wiley & Sons, 1998.
7. A. J. Fenn et al., “The Development of Phased-Array Radar Technology,” *MIT Lincoln Laboratory Journal*, Vol. 12, No. 2, 2000.
8. D. Heo et al., “Integrated Eight Element Ku-Band Transmit/receive Beamformer Chipset for Low-cost Commercial Phased Array Antennas,” IEEE International Symposium on Phased Array Systems and Technology, October 2010.
9. G. Rebeiz, “Effect of Output-to-Input Coupling on Phased Arrays,” Personal Communication, May 2014.

Ian Gresham *is a technology fellow at Anokiwave, where he serves as IC system architect. Gresham has over 25 years experience in radar, telecommunications and semiconductor technology and has contributed to the product and technology development at NXP and M/A-COM. He holds bachelor's and doctorate degrees from the University of Leeds and is a fellow of the IEEE.*

Rob McMorrow *has over 20 years experience in RF circuit design, particularly power amplifiers. Before joining Anokiwave, he was co-founder and chief technical officer of Star RF/Xikota Devices, formed to develop CMOS PAs for wireless handsets. His design expertise has also served Raytheon, Skyworks and Analog Devices. McMorrow received his bachelor's and master's degrees from Cornell University.*

David Corman *is chief systems architect at Anokiwave, applying his 34 years experience in RF system, module and RFIC/MMIC design. Previously, he co-founded US Monolithics and spent 15 years at Motorola. At Motorola, he was the architect and lead technologist for the Iridium Block 1 space-based K- and Ka-Band electronics suite. His contributions have been recognized with over 40 patents. Corman received his bachelor's degree from the University of Kansas and a master's from Arizona State University.*

Nitin Jain *founded Anokiwave in 2000, where he designs and consults with customers. Before starting Anokiwave, he was at M/A-COM, where his contributions included leading the technical development of a 77 GHz automotive radar module. Jain has been awarded 20 U.S. patents and has written more than 37 papers and articles. He holds a bachelor's degree from the Indian Institute of Technology and master's and doctorate degrees from Rensselaer Polytechnic Institute.*

Scan page using layar app

INVITED PAPER

Flexible Testbed for 5G Waveform Generation and Analysis

Greg Jue
Keysight Technologies Inc., Santa Rosa, Calif.

While LTE and LTE-Advanced are still being deployed, research into next generation wireless networks is already in high gear. That next generation – 5G – will likely comprise a dense, highly integrated network of small cells supporting peak data rates of up to 10 Gbps and 1 ms or less roundtrip latencies, while utilizing a number of different air interfaces at both microwave and millimeter wave frequencies. The combined network may be able to support everything from simple machine-to-machine (M2M) devices to immersive virtual reality streaming. While that bodes well for an end user experience, it presents some interesting challenges for those engineers developing 5G systems.

Making the leap from prediction to practical implementation starts with the creation, generation and analysis of prototype signals. As there is no 5G standard at this time, no physical layer waveforms have yet been defined. Although there is a lack of consensus on 5G waveforms, filter bank multi-carrier (FBMC), universal filtered multi-carrier (UFMC) and orthogonal frequency-division multiplexing (OFDM) waveforms are being considered. Other potential candidates include waveforms at sub-6 GHz frequencies and those at microwave and millimeter wave (mmWave), which may involve wide bandwidths of up to 2 GHz. The number and variety of waveforms, frequencies and bandwidths being researched introduce new test challenges for 5G signal generation and analysis.

Key to overcoming these challenges is flexibility during 5G research and early testing. Engineers must have the ability to perform "what-if" analyses while they are evaluating early concepts and new candidate 5G waveforms. Without this ability, the risk of choosing the wrong path and not discovering issues until much later in the development cycle – when it is much more costly and time consuming to change – can increase. Flexibility, especially with signal creation and signal analysis tools, can be especially important, as they enable rapid changes in direction as strong 5G waveform candidates emerge. Engineers also need the flexibility to use a wide range of modulation bandwidths (from several megahertz to a few gigahertz) and frequency bands (from RF to microwave to mmWave).

To address these challenges, engineers would ideally like to combine off-the-shelf hardware and software to create a flexible 5G waveform generation and analysis test platform, such as Keysight's 5G waveform generation and analysis testbed reference solution (see ***Figure 1***). The testbed reference solution provides flexibility through its software and hardware elements. In the software, flexibility ensures that engineers can generate and analyze various types of 5G candidate and custom waveforms. With the hardware, both flexibility and scalability work together to give engineers the ability to generate and analyze signals from RF to mmWave frequencies with up to 2 GHz bandwidth.

To generate wideband test signals with up to 2 GHz of modulation bandwidth at frequencies up to 44 GHz, the solution employs a precision arbitrary waveform generator (ARB) and vector signal generator, with wideband I/Q inputs, running signal creation software. Higher frequencies can be achieved through the use of an up-converter. This combination of hardware and software enables 5G candidate waveforms such as custom FBMC, OFDM and single-carrier to be generated. Integration of system-level design software with hardware further enables custom or proprietary algorithms and "what-if" scenarios to be evaluated, such as the coexistence of an LTE signal in the presence of an FBMC signal.

The testbed reference solution can also be used to demodulate and analyze test signals. In this case, 89600 VSA software is typically employed with the simulation software or on a number of different hardware options, including a signal analyzer, oscilloscope or PC that controls a variety of instruments or digitizers.

To illustrate the viability of this type of testbed reference solution, two test cases will be examined: a ~1 GHz wide custom OFDM signal at 28 GHz and a 2 GHz single-carrier signal at 73 GHz.

28 GHz WIDEBAND OFDM SIGNAL

For this case, the testbed reference solution combines a precision AWG with a vector signal generator with wideband I/Q inputs to produce wideband microwave test signals up to 44 GHz. Signal creation software enables the custom OFDM waveform to be created with approximately 1 GHz modulation bandwidth at 28 GHz (see ***Figure 2***). Resource-mapping parameters were set for the preamble, pilot and data subcarriers, including the location and boosting of each resource block. I/Q values were set for the preamble, modulation and payload for pilot and data. The waveform is generated, then read into the AWG and played out using the AWG's front panel software. The I/Q outputs of the AWG are fed into the wideband I/Q inputs on the vector PSG, and the PSG modulates the I/Q waveforms on a 28 GHz carrier. The test signal from the PSG RF output is analyzed using a 63 GHz high-performance oscilloscope with 89600 VSA software.

The resulting test signal measurement with the 89600 VSA software (see ***Figure 3***) comprises a six-trace display that shows (clockwise from upper left) the constellation, error vector magnitude (EVM) versus subcarrier, search time, OFDM equalizer channel frequency response, error summary and the ~1 GHz spectrum at the 28 GHz center frequency.

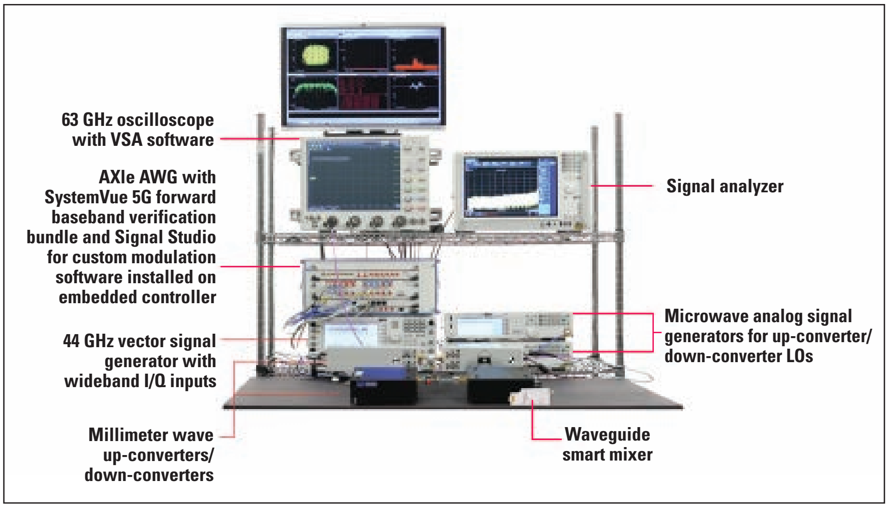

▲ *Fig. 1 Flexible 5G waveform generation and analysis testbed.*

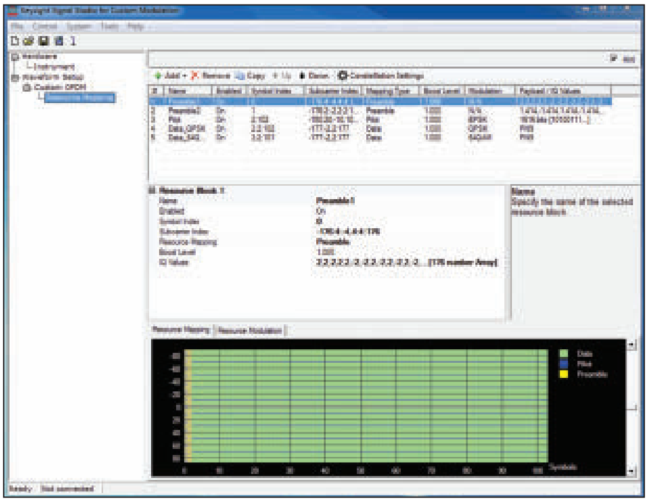

▲ *Fig. 2 Signal creation software for creating custom, wide bandwidth OFDM signals.*

▲ *Fig. 3 Custom OFDM signal with ~1 GHz bandwidth at 28 GHz.*

SINGLE CARRIER SIGNAL AT 73 GHz

For this case, the testbed reference solution configuration is extended to 73 GHz using a mmWave up-converter for signal generation and either a mmWave down-converter or waveguide smart mixer for signal analysis. The configuration shown in ***Figure 4*** uses a microwave signal generator to provide the LO for the mmWave up-converter. A mmWave amplifier and filter at the up-converter output may be added to boost power and filter the spectrum. A waveguide smart mixer is used for signal analysis from 60 to 90 GHz, combined with a signal analyzer and oscilloscope. The waveguide smart mixer is connected to the output of the mmWave up-converter, and the IF output is fed into the signal analyzer for spectrum analysis. The auxiliary IF output is fed into the oscilloscope for wide bandwidth demodulation analysis with the VSA software.

At these frequencies and bandwidths, linear amplitude and phase er-

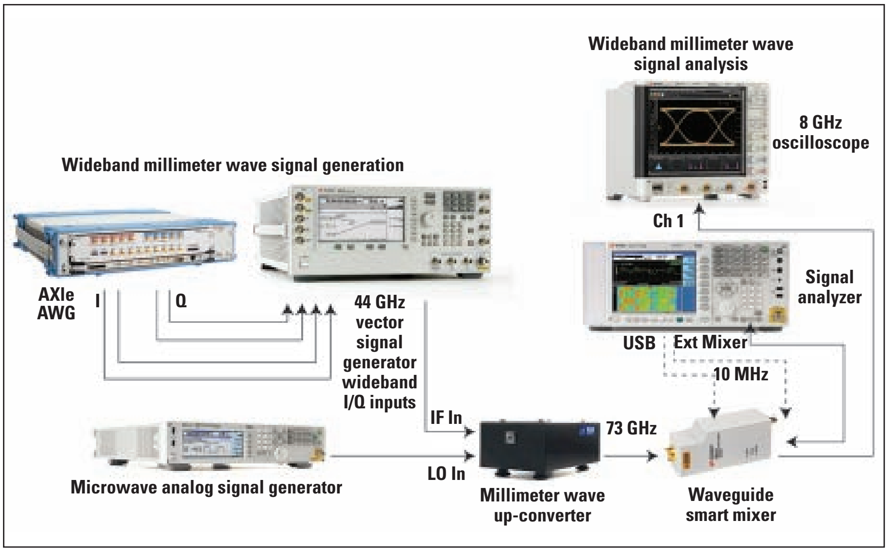

▲ *Fig. 4 Example hardware setup for waveform generation and analysis at 73 GHz (mmWave amplifier and filter not shown).*

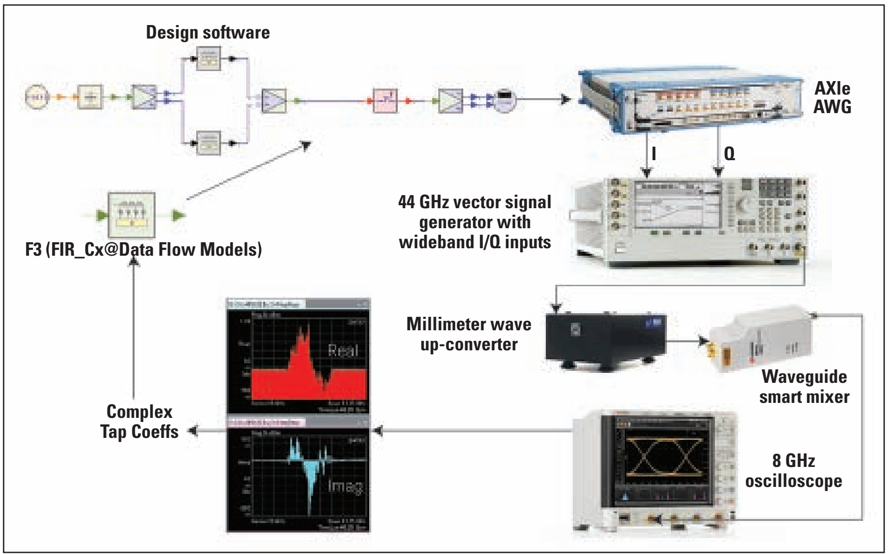

▲ *Fig. 5 Integrating design software and test equipment to correct for linear amplitude and phase errors in the test signal (mmWave amplifier and filter not shown).*

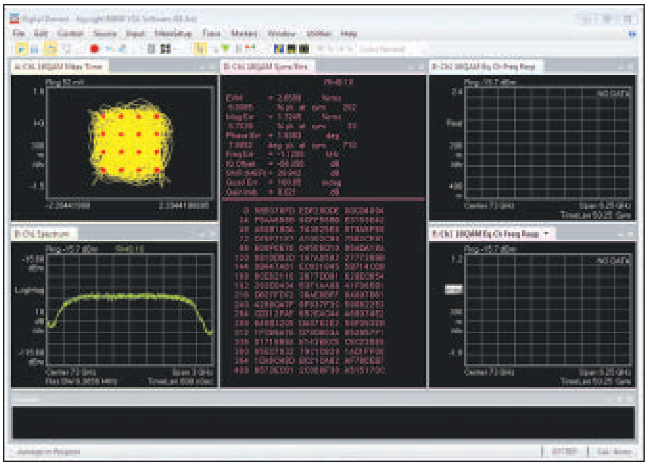

▲ *Fig. 6 Demodulating a 73 GHz waveform with 2 GHz of modulation bandwidth. Constellation maximum used as the EVM normalization reference.*

rors may be caused within the signal chain by the AWG, vector signal generator, up-converter, waveguide smart mixer, cables/interconnects and signal analyzer. These were reduced by deriving the necessary vector corrections using the adaptive equalizer in the VSA software. The equalizer produces a complex-valued frequency response that can be used to minimize amplitude and phase errors. This is done by reading the frequency response into the system-level design software used to generate the wideband waveform, and then using it to pre-correct the waveform response (see ***Figure 5***).

Figure 6 shows the demodulation analysis of the vector-corrected waveform at 73 GHz, with 2 GHz modulation bandwidth. Demodulating a 2 GHz wideband signal is typically quite difficult without adaptive equalization, due to hardware impairments across the wide bandwidth. However, in this example the linear amplitude and phase errors were corrected in simulation to generate a waveform that produced a low EVM without adaptive equalization.

CONCLUSION

The development of 5G includes an aggressive set of characteristics that will be difficult to achieve. A high degree of flexibility is needed to help researchers and engineers address these challenges and quickly respond to changes in direction as 5G evolves.

Test systems such as the 5G waveform generation and analysis reference solution combine hardware and software to create a flexible 5G waveform generation and analysis platform. This enables engineers and researchers to generate and analyze emerging 5G candidate waveforms. The software elements for the testbed provide flexibility in the types of 5G candidate waveforms being generated and analyzed. The hardware elements for the testbed provide flexibility and scalability from RF to microwave to mmWave and modulation bandwidths up to 2 GHz. ■

Greg Jue *is an applications development engineer working on 5G applications at Keysight Technologies. He has worked in Keysight's aerospace and defense applications team, the high performance oscilloscopes team and at EEsof, specializing in 802.11ac, LTE, WiMAX, aerospace and defense and software-defined radio applications. Jue wrote the design simulation section in Agilent Technologies' LTE book and has authored numerous articles, presentations, application notes and whitepapers. Before joining HP/Agilent, he worked on the system design for the Deep Space Network at the Jet Propulsion Laboratory.*

INVITED PAPER

Expanding Mobile Capacity: The Evolution to LTE-U and LAA

Andreas Roessler
Rohde & Schwarz, Munich, Germany

As mobile operators seek additional spectrum to handle the exponential growth in data traffic, the unlicensed 5 GHz bands offer additional spectrum to increase system capacity at literally no cost. Standards development to share the spectrum is well underway, known in the industry as LTE-U and LAA. This article explores the basic principles behind LTE-U and LAA, the approach to ensure coexistence and fair sharing, and implementation challenges.

Due to the ongoing transition from voice-centric mobile phones to smartphones and tablets – greatly accelerated by the launch of LTE networks beginning in 2009 – mobile broadband data consumption has increased exponentially over the past five years. Global mobile data traffic grew 69 percent in 2014 alone and reached 2.5 exabytes per month, up from 1.5 exabytes per month in 2013. Additional growth of 59 percent is forecast for 2015, reaching 4.2 exabytes per month. Video streaming is the dominant traffic type and accounted for more than 55 percent of all mobile data traffic in 2014. Such ongoing exponential growth represents quite a challenge for mobile network operators worldwide.

Service providers must efficiently use the spectrum available to them to deliver an excellent user experience while offering high data rates on an average basis to every subscriber. LTE is the technology of choice; however, spectrum is not an infinite resource. Over recent years, service providers have invested billions of dollars on a global scale to increase their spectrum holdings and, thus, their system capacity. However, only a limited amount of frequencies are available that local regulators can auction off to service providers, leading to tough competition as well as bidding wars in extreme cases to acquire additional licenses.

Due to this shortage, alternatives are required. One very promising alternative is to take advantage of unlicensed spectrum, such as the industrial, scientific and medical (ISM) frequency bands – especially the underutilized 5 GHz frequency band. Opportunistic usage of the spectrum, while deploying LTE component carriers in this frequency band, allows network operators to increase their system capacity while adding additional spectrum

resources at literally no cost. This alternative is known across the industry as LTE in unlicensed spectrum, or LTE-U. This approach has gained significant momentum, especially in the United States.

Accordingly, the 3GPP, the standardization body behind LTE, took up the challenge of enhancing the technology while adding the required functionality to support LTE-U. The feature is currently being standardized as licensed assisted access (LAA) using LTE. It will be added with Release 13, which should be finalized in March 2016. Of course, there is no free lunch, and everything has its price. Coexistence and fair sharing of the spectrum resource among LTE-U operators and, more importantly, with existing technologies such as Wi-Fi are important prerequisites to the success of LTE-U/LAA.

5 GHZ SPECTRUM REGULATION

The 5 GHz spectrum is regulated in a similar manner throughout the world, but additional rules do apply in the different regions. Frequency regulation from a global perspective is administered by the International Telecommunication Union (ITU) on a regional basis. There are three regions defined. ITU Region 1 is primarily Europe; ITU Region 2 is America, including the United States, Canada and Brazil, for example; and ITU Region 3 is Asia with China, Japan and South Korea. Countries belonging to any of these regions typically adhere to the overall concept for that region; however, there can be additional regulations in place locally that apply to certain parts of the spectrum. The regulatory aspects for the 5 GHz spectrum in the U.S. are considered in this article, since there is a very strong interest in LTE-U and LAA that is driven by local tier one operators.

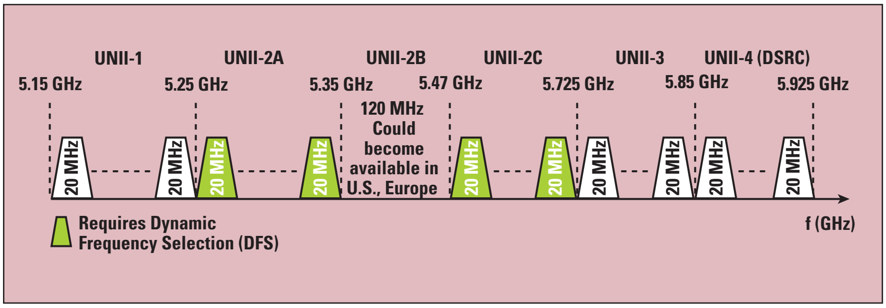

Fig. 1 5 GHz spectrum allocation.

Figure 1 shows the spectrum allocation in the U.S. The spectrum between 5150 and 5925 MHz is divided into four domains that are designated UNII-1 to UNII-4, where UNII stands for unlicensed national information infrastructure. For the four domains, different regulatory rules apply, for example, the allowed maximum conducted output power, the peak power spectral density (PSD) and out-of-band (OoB) emissions. ***Table 1*** shows the requirements set by the Federal Communications Commission (FCC), the regulatory authority in the U.S.[1]

As can be gathered from Table 1, UNII-2 devices need to support transmit power control (TPC) as well as dynamic frequency selection (DFS); (see Figure 1). In contrast, UNII-1

TABLE 1

TRANSMIT POWER REQUIREMENTS FOR UNII DEVICES OPERATING IN THE U.S.[1]

Frequency Band		UNII-1 5.15 – 5.25 GHz	UNII-2A 5.25 – 5.35 GHz	UNII-2C 5.47 – 5.725 GHz	UNII-3 5.725 – 5.85 GHz	Comments
Maximum Conducted Output Power (dBm) <min (a,b)	a	eNB: 30 UE: 24	24	24	30	
	b		11+10log(B)	11+10log(B)		B is the 26 dB emission bandwidth
Peak Power Spectral Density (dBm/MHz)		eNB: 17 UE: 11	11	11	30 dBm in 500 kHz	
Assumed Antenna Gain (dBi)		6	6	6	6	Peak power is reduced by G–6 dB for directional antennas with gain > 6 dBi
Out-of-Band (OoB) Emissions	Frequency Support (GHz)	Outside 5.15 – 5.35	Outside 5.15 – 5.35	Outside 5.47 – 5.725	Outside 5.715 – 5.865	
	EIRP (dBm/MHz)	-27	-27	-27	-27	Resolution bandwidth = 1 MHz
	Frequency Support (GHz)				5.715-5.725 5.85 – 5.86	
	EIRP (dBm/MHz)				-17	
Transmit Power Control (TPC)		N/A	TPC to 6 dB below a mean EIRP of 30 dBm. No TPC for mean EIRP < 27 dBm		N/A	

and UNII-3 do not require this additional mechanism to ensure coexistence with other systems, thereby making the lower and upper portion of the spectrum the first targeted frequencies that will be used by LTE-U and LAA. Consequently, two new frequency bands were defined by the 3GPP as Band 252 and Band 255, which correspond to UNII-1 and UNII-3, respectively. Note that the channel raster definition for these two bands follows the Wi-Fi channel assignment to avoid in-channel interference.

With the band definition, the 3GPP is acknowledging the initial work that has been done within an industry alliance, called the LTE-U Forum, which was forged to accelerate the time to market for LTE-U. The founding members of the LTE-U Forum were Verizon Wireless, Qualcomm, Ericsson, Alcatel-Lucent and Samsung. These key players in the wireless industry have agreed on coexistence aspects to allow fair sharing of the spectrum resource with other LTE-U operators and technologies such as Wi-Fi. Furthermore, they agreed on a set of specifications to define the minimum requirements for handsets and base stations supporting LTE-U.

For example, the minimum requirements for an eNB (LTE base station) are based on the 3GPP's technical specification (TS) 36.104. This document takes the limits and tolerances that are provided within TS 36.104 for RF measurements, such as adjacent channel leakage power ratio (ACLR) or spectrum emission mask (SEM), and adapts them for base stations that support LTE-U in terms of the regulatory aspects. ***Figure 2*** shows an adapted spectrum emission mask (SEM) measurement on an LTE-U capable base station operating in frequency band 255 (UNII-3). The measurement is in line with the LTE-U eNB minimum requirements specification.[2]

To distinguish the work done by the LTE-U Forum from that of the 3GPP, from a forum perspective, LTE-U is defined to use bands 252 and 255 as a supplemental downlink only. The LAA work item also defines the anchor carrier or primary component carrier (PCC) for the communications link to reside in a licensed frequency band but does not exclude the use of the 5 GHz spectrum for uplink carrier aggregation at a later stage. For the moment, the 3GPP is also considering the (secondary) component carrier placed in the 5 GHz bands solely as a transmission resource.[3]

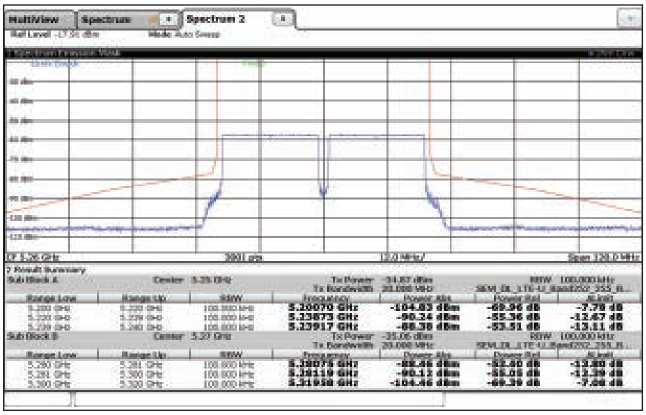

▲ *Fig. 2 SEM measurement using the R&S®FSW signal and spectrum analyzer in line with the LTE-U eNB minimum requirements specification.*

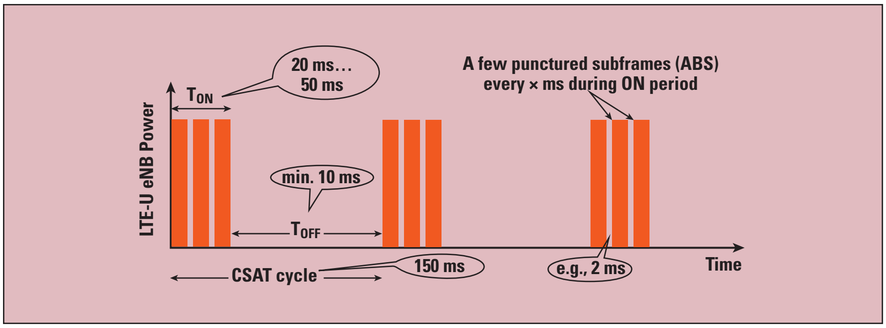

▲ *Fig. 3 LTE-U base stations use CSAT to ensure fair spectrum sharing with other LTE-U operators and Wi-Fi.*

ENSURING COEXISTENCE

The LTE-U Forum members have agreed on a two-step approach to ensure coexistence with other technologies and LTE-U operators, along with fair sharing of the spectrum resource with existing technologies. First, this is based on smart channel selection during the initial boot-up phase, which is then continued dynamically during operation. In other words, an LTE-U capable base station (similar to a Wi-Fi access point) periodically monitors the frequency band and selects its channel based on channel quality measurements and input parameters such as traffic load. A 'channel penalty' function has been proposed that has multiple input parameters with variable weighting factors. Based on the measurements and weighting factors, a penalty for each potential channel is determined. The channel with the lowest penalty is selected and a 20 MHz LTE component carrier is transmitted on this frequency channel. A terminal that supports LTE-U is informed about the exact carrier frequency via the defined signaling methods for carrier aggregation and can thus access that component carrier.

As of now, aggregation of up to three component carriers is foreseen. One is in a licensed frequency band that could have any bandwidth depending on the spectrum of the respective operator. In addition, there can be up to two 20 MHz component carriers in the unlicensed frequency band. Such carriers are always 20 MHz wide – no more and no less due to the Wi-Fi channel definition, where the minimum bandwidth is 20 MHz. In total, there could be an aggregated transmission bandwidth of up to 60 MHz, including 2 × 2 MIMO operation per component carrier, and a maximum peak data rate of 450 Mbps.

After initial channel selection, the LTE-U capable base station must use carrier sensitive adaptive transmission (CSAT) to ensure fair sharing with other LTE-U operators using the spectrum and Wi-Fi. The basic principle behind CSAT is to define a cycle with a duration of some milliseconds that is divided into an "on" period and an "off" period. The length of the cycle and thus the duration of the on and off periods are dynamically adaptable based on the traffic situation (see ***Figure 3***). If there is a heavy load on the selected channel, when many Wi-Fi access points and other LTE-U base stations are active, then the CSAT cycle might be long, up to 150 ms, and the on period short, for example only 20 ms. If the channel is not heavily occupied, a shorter CSAT cycle might be appropriate with a longer on period and therefore a shorter off period. Note that the values shown in Figure 3 were suggestions by LTE-U Forum members, presented at a workshop in May 2015.

During the on period of the CSAT cycle, a few subframes are periodically punctured and configured as almost blank subframes (ABS). The actual quantity depends on the duration of the on period and, thus, on the traffic load. The puncturing of subframes is intended to ensure that latency-sensitive applications that run over Wi-Fi, such as voice over Wi-Fi (VoWi-Fi), can still function once LTE-U is operational.

Besides testing the RF conformance of LTE-U capable base stations by measuring the transmission power, SEM and ACLR, it is important to test handset performance and coexistence. To demonstrate LTE-U performance, a setup that was featured at Mobile World Congress 2015 was used to emulate and aggregate three LTE component carriers with a bandwidth of 20 MHz each and 2×2 MIMO. Two of the component carriers were placed in a licensed frequency band, and the other component carrier was placed in the UNII-3 domain of the 5 GHz spectrum. Aggregating these three carriers achieved a maximum data rate of 450 Mbps. The demonstration involved a maximum throughput test to verify that the device under test was capable of handling this high data rate.[4] To ensure coexistence, it was also important to verify that the device was able to support CSAT.

OUTLOOK

The 3GPP is standardizing LTE-U functionality known as LAA. Part of the standardization involves integrating listen before talk (LBT) functionality, which is required in Europe and Japan to use the 5 GHz spectrum. A device that wants to utilize the spectrum must always sense the channel first before starting to transmit. At this time, the standardized LBT functionality is based solely on energy detection.

LTE-U is currently a hot topic in the wireless industry. The feature provides an attractive alternative for network operators who want additional spectrum to increase their system capacity. Fair sharing of the resource among operators and existing technologies such as Wi-Fi is key to the success of LTE-U. ■

References

1. 3GPP TR 36.889 V13.0.0, 3rd Generation Partnership Project; Technical Specification Group Radio Access Network; Study on Licensed-Assisted Access to Unlicensed Spectrum; (Release 13), June 2015.
2. eNB Minimum Requirements for LTE-U SDL V1.0, LTE-U Forum, http://lteuforum.org/uploads/3/5/6/8/3568127/lte-u_forum_enb_minimum_requirements_for_lte_u_sdl_v1.0.pdf, February 2015.
3. 3GPP Work Item for "Licensed-Assisted Access using LTE," www.3gpp.org/ftp/tsg_ran/TSG_RAN/TSGR_68/Docs/RP-151045.zip.
4. LTU-U Maximum Throughput demonstration at Mobile World Congress by Rohde & Schwarz, https://www.youtube.com/watch?v=l-e0IllyxnU, March 2015.

INVITED PAPER

60 GHz Backhaul Links Ready to Boost Cellular Capacity

John Kilpatrick and Robbie Shergill
Analog Devices, Norwood, Mass.
Manish Sinha
Xilinx Inc., San Jose, Calif.

The ever-increasing demand for data on the world's cellular networks has operators searching for ways to increase capacity 5000× by 2030.[1] Getting there will require a 5× increase in channel performance, a 20× increase in allocated spectrum and a 50× increase in the number of cell sites. Many of these new cells will be placed indoors, where the majority of traffic originates, and fiber is the top choice to funnel the traffic back into the network. Yet there are many outdoor locations where fiber is not available or is too expensive to connect; for these situations, wireless backhaul is the most viable alternative.

Unlicensed spectrum at 5 GHz is available and does not require a line-of-sight (LOS) path. However, bandwidth is limited and interference from other users of this spectrum is almost guaranteed, due to heavy traffic and wide antenna patterns. 60 GHz is emerging as a leading contender to provide these backhaul links for the thousands of outdoor cells that will be required to meet capacity demands. This spectrum is also unlicensed. Unlike frequencies below 6 GHz, it contains up to 9 GHz of available bandwidth. Moreover, the high frequency allows for very narrow and focused antenna patterns that are somewhat immune to interference; however, they do require LOS paths.

Modems based on FPGAs and systems on a chip (SoC) are increasingly used in wireless backhaul solutions, since platforms using them can be modular and customizable, reducing the total cost of ownership for OEMs. For the radio portion of these links, transceivers have been integrated into silicon ICs and assembled in low cost, surface-mount packages. Commercial parts are now available to build a complete two-way data link at 60 GHz, filling each of the functional blocks in ***Figure 1***. Developed by Xilinx and Hittite Microwave (now Analog Devices), the design includes a Xilinx modem and Analog Devices millimeter wave radio. This link meets the performance and flexibility requirements of the small cell backhaul market.

As shown in Figure 1, two nodes are required to create the link. Each node contains a transmitter with a modulator and its associated analog chain and a receiver with a demodulator and its associated analog chain. The modem card is integrated with analog and discrete devices. It contains oscillators to ensure the accuracy of frequency synthesis, and all the digital functions are executed in an FPGA or SoC. This single-carrier modem core supports modulations from QPSK to 256 QAM in channel bandwidths up to 500 MHz, achieving data rates as high as 3.5 Gbps. The modem supports both frequency-division duplex (FDD) and time-division duplex (TDD) transmission. Robust modem design techniques reduce the phase noise implications of the local oscillators. Powerful low-density parity check (LDPC) coding is included for improved performance and link budget.

MILLIMETER WAVE MODEM

The millimeter wave modem enables infrastructure suppliers to develop flexible, cost-optimized and customizable links for their wireless backhaul networks. The modem is fully adaptive, low power and small, and can be used to deploy indoor and full outdoor point-to-point links, as well as point-to-multipoint links. The solution allows operators to build scalable and field-upgradable systems.

Figure 2 shows a functional block diagram of the digital modem, which is implemented as an SoC. Besides the programmable logic (PL), the platform's scalable processing system (PS) contains dual ARM Cortex-A9 cores with integrated memory controllers and multistandard I/Os for peripherals. The SoC platform is used to perform various data and control functions and to enable hardware acceleration. An integrated millimeter wave modem complete with PHY, controller, system interfaces and packet processor is included.

Based on the required architecture, different modules can be inserted, updated or removed. For example, an XPIC combiner could be implemented to enable the modem to be used in a cross-polarization mode with another modem. The solution is implemented in the PL, where serializer/deserializer (SerDes) and I/Os are used for various data path interfaces, such as between the modem and packet processor, the packet processor and memory, inter-modem or DAC/ADC.

Other important features of the modem IP include:

- Automatic hitless and errorless state switching through adaptive coding and modulation (ACM) to keep the link operational
- Adaptive digital closed-loop predistortion (DPD), to improve RF power amplifier efficiency and linearity
- Synchronous Ethernet (SyncE), to maintain clock synchronization and
- Reed Solomon or LDPC forward error correction (FEC), based on the design requirements.

LDPC FEC is the default choice for wireless backhaul applications, while Reed Solomon is preferred for low-latency applications such as front-haul. LDPC implementation is highly optimized and exploits FPGA parallelism for computations done by the encoders and decoders. The result is noticeable SNR gains. Different levels of parallelism are applied by varying the number of iterations of the LDPC core, which optimizes the size and power of the decoder. The design can also be modeled based on channel bandwidth and throughput constraints.

This modem solution comes with a graphical user interface (GUI) for both display and debug. It is capable of high level functions such as channel bandwidth and modulation selection as well as low level ones such as setting hardware registers. To achieve 3.5 Gbps throughput, the modem IP runs at a 440 MHz clock rate. It uses five gigabit transceivers (GT) for connectivity interfaces to support the ADCs and DACs and a

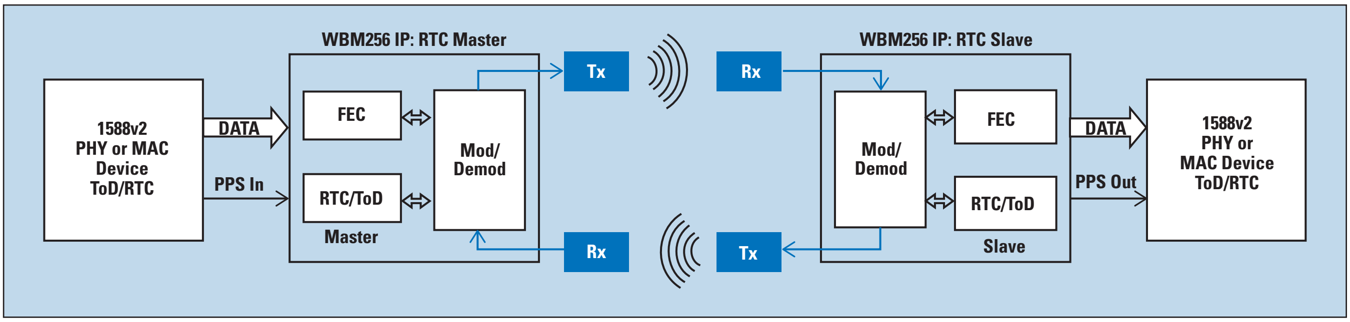

▲ *Fig. 1 Functional block diagram of the two-way 60 GHz link.*

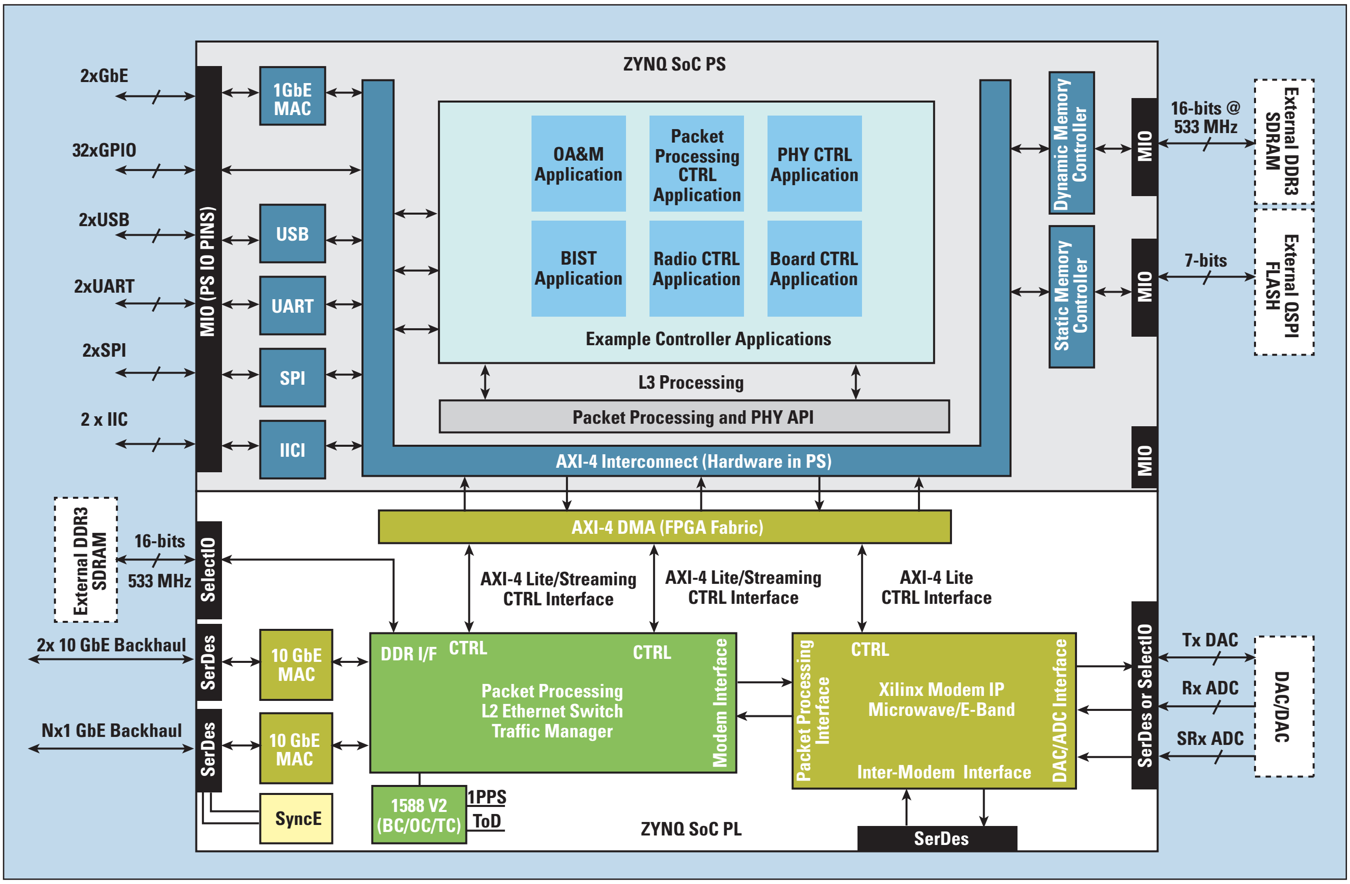

▲ *Fig. 2 The wireless digital modem is implemented with a programmable SoC.*

few more GTs for 10 GbE payloads and CPRI interfaces.

MILLIMETER WAVE TRANSCEIVER

A second-generation SiGe chipset was optimized for 60 GHz small cell backhaul applications. The transmitter chip is a complete analog baseband to millimeter wave up-converter. An improved frequency synthesizer covers 57 to 66 GHz in 250 MHz steps, with low phase noise that can support modulations up to at least 64 QAM. The output power was increased to roughly 16 dBm linear, and an integrated power detector monitors the output power to maintain the output within regulatory limits. The transmitter chip offers either analog or digital control of the IF and RF gains. Analog gain control is sometimes needed when using higher-order modulation, since discrete gain changes can be mistaken for amplitude modulation, leading to bit errors. A built-in serial peripheral interface (SPI) supports digital gain control.

For applications requiring even higher-order modulation in narrow channels, an external PLL/VCO with lower phase noise can be injected into the transmitter, bypassing the internal synthesizer. ***Figure 3*** shows a block diagram of the transmitter chip, which supports up to 1.8 GHz of bandwidth. An MSK modulator option enables low cost data transmissions up to 1.8 Gbps without the need for expensive and power-hungry DACs.

A receiver chip complements the transmitter IC (see ***Figure 4***) and is, likewise, optimized to meet the demanding requirements of small cell backhaul applications. The receiver features a significant increase in the input P_{1dB} to -20 dBm and IIP3 to -9 dBm to handle short-range links, where the high gain of the dish antennas leads to high signal levels at the receiver input. Other key features include a low 6 dB noise figure at maximum gain, adjustable lowpass and highpass baseband filters, either analog or digital control of the IF and RF gains and the same new synthesizer design found in the transmitter chip, to support 64 QAM modulation over 57 to 66 GHz. The receiver also contains an AM detector to demodulate amplitude modulation such as on/off keying (OOK) and an FM discriminator to demodulate simple FM or MSK modulation. This

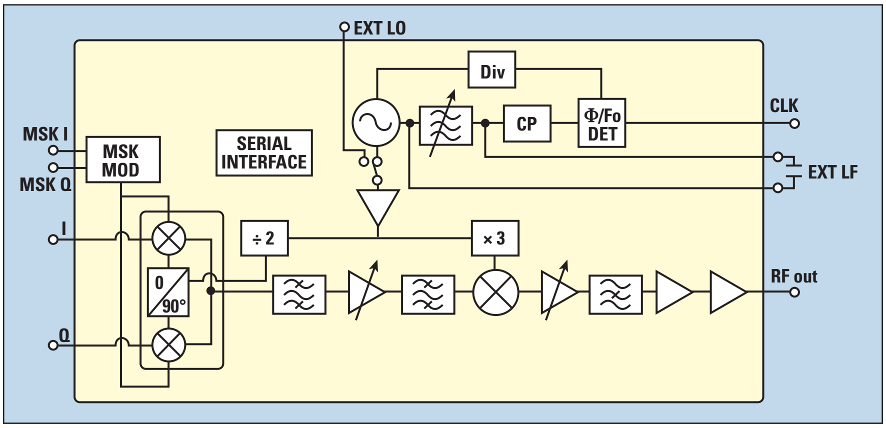

▲ *Fig. 3 Functional block diagram of the 60 GHz transmitter IC.*

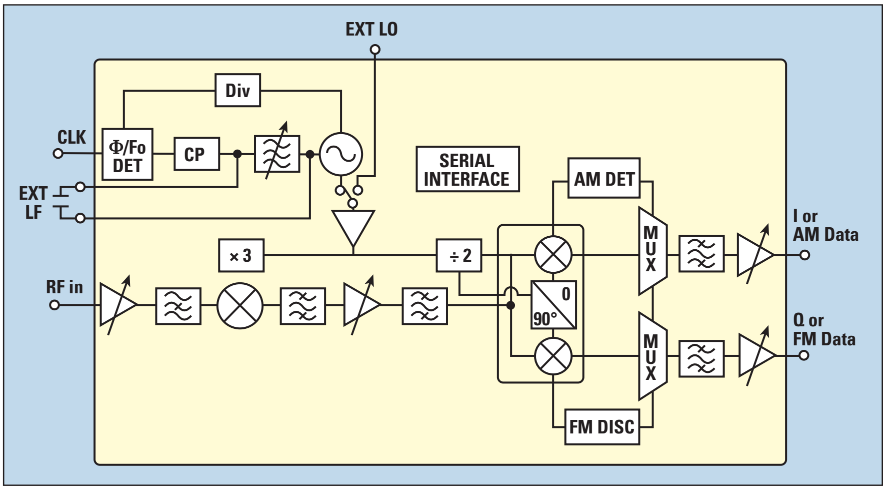

▲ *Fig. 4 Functional block diagram of the 60 GHz receiver IC.*

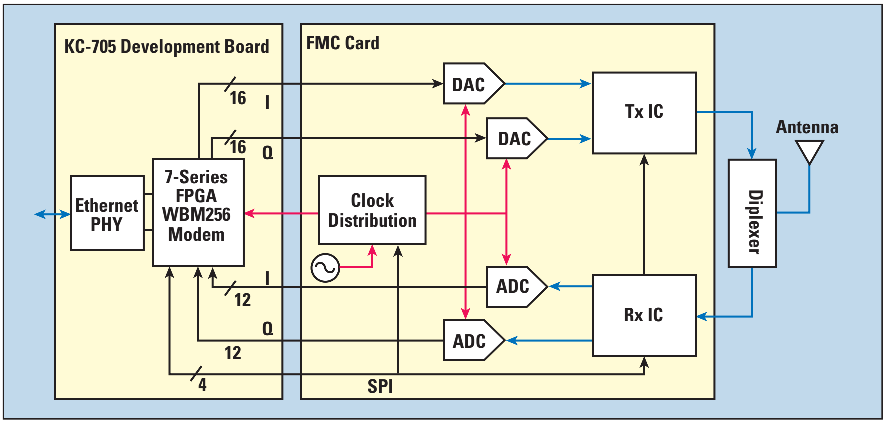

▲ *Fig. 5 A reference design for the 60 GHz link based on Xilinx and Analog Devices ICs.*

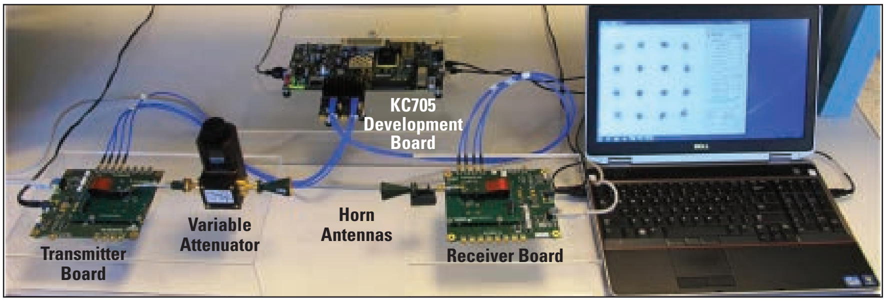

▲ *Fig. 6 60 GHz link demonstration platform.*

is in addition to the I/Q demodulator that is used to recover the quadrature baseband outputs for QPSK and more complex QAM modulation.

Both transmitter and receiver ICs come in a 4 × 6 mm wafer-level BGA package. Surface-mount packaging supports low cost manufacturing of radio boards for backhaul applications.

Figure 5 shows a block diagram of an the millimeter wave modem and radio system. In addition to the FPGA, modem software and millimeter wave chipset, the design contains a dual-channel, 12-bit 1 GSPS ADC; a quad-channel, 16-bit, up to 2.8 GSPS Tx DAC; and an ultra-low jitter clock synthesizer, with support for the JESD204B serial data interface employed on both the ADC and DAC ICs. A demonstration platform (see ***Figure 6***) was jointly created by Xilinx and Analog Devices. It includes the FPGA-based modem on a Xilinx development board, a standard FMC board containing ADCs, DACs and clock and two radio module evaluation boards. The platform includes a laptop for modem control and visual display and a variable RF attenuator to replicate the path loss of a typical millimeter wave link. The FPGA on the development board executes the WBM256 modem firmware IP. A standard FMC mezzanine connector on the development board connects to the baseband and millimeter wave radio boards. The millimeter wave modules snap onto the baseband board. The modules have MMPX connectors for the 60 GHz interfaces and SMA connectors for optional use of an external local oscillator. This platform contains all the hardware and software needed to demonstrate point-to-point backhaul connections of up to 1.1 Gbps in 250 MHz channels for each direction of an FDD link.

DESIGN CONSIDERATIONS

The experience developing the modem, transceivers and demonstration platform yielded the following considerations for designers:

Since they're highly modular and customizable, FPGAs can reduce the cost to build platforms for wireless backhaul. When choosing commercial parts for a millimeter wave modem solution for small cell, select power-efficient FPGAs/SoCs and high performing wideband IP cores. High speed is also a factor to consider when selecting GTs for wideband communications and switching functions. Look for a solution that can scale to support multiple product variations on the same hardware platform, from lower end, small cell backhaul radios that operate at a few hundred megabits per second to high performance systems carrying 3.5 Gbps.

For the radio, transceiver ICs in surface mount packages will lower the cost of manufacturing. Parts currently on the market will meet the power, size, flexibility and functionality requirements for small cell wireless backhaul. The high-performing data converters and clock-management ICs that are required to complete a wireless backhaul link are also commercially available.■

Reference

1. "Evolutionary and Disruptive Visions Towards Ultra High Capacity Networks," *IWPC*, April 2014.

INVITED PAPER

Multiplexers in Mobile Handsets with LTE-Advanced Carrier Aggregation

Uli B. Koelle
Avago Technologies, San Jose, Calif.

In many parts of the world, smartphones have become an integral part of everyday life, and many users rely on their handsets as an easy way for going online. In the U.S., it is reported that in early 2011, one in three Americans owned a smartphone. As of 2015, that number has almost doubled.[1] Projections indicate that in 2016 smartphone penetration will exceed 80 percent in the U.S.[2] This continuous growth of smartphone popularity, and the expansion of its user base feeds the need for increased wireless data traffic, which has to be met with an increase in available bandwidth. The 3GPP standards body for mobile broadband specifies the spectrum of bands that can be used in wireless communications. Since the wireless spectrum is already crowded, and new chunks of wireless spectrum are hard to come by, 3GPP's LTE-Advanced specifications identify carrier aggregation (CA) as one means to increase bandwidth over existing LTE frequency bands.[3]

With LTE, data traffic is aggregated in component carriers (CC) which are blocks of frequency spectrum 1.4, 5, 10 or 20 MHz wide. To increase the bit rate, CA means that up to five CCs can be aggregated, either within the same band or across different frequency bands. The number of downlink CCs must always equal or be greater than the number of uplink CCs. Since most of the wireless traffic demand is presently in the downlink (DL) direction, only one uplink (UL) CC is used, limiting carrier aggregation to the DL direction.

All smartphones on the market today already include the capability to transmit and receive on different frequency bands, for roaming purposes. However, enabling simultaneous operation of two separate LTE bands for CA puts additional constraints on the phone's hardware components and data traffic management. In particular, inter-band CA with two frequency division duplex (FDD) LTE bands means that each transmit band now has two equally valid receive bands associated with it.

MULTIPLEXERS

Smartphones combine a lot of functionality into a relatively small package, and the size of any component inside the phone is limited. The RF front-end in a handset comprises all components between the antenna and the baseband/transceiver chips, such as frequency filtering devices, switches, power amplifiers, LNAs and a number of matching and routing elements. For any FDD band, a duplexer comprises two RF filters which ensure that the uplink transmit signal (Tx) does not interfere with the downlink reception (Rx). Integrating multiple non-overlapping filter bands into a single module (multiplexer) can reduce component count and the size of the phone's RF

HUBER+SUHNER
Excellence in Connectivity Solutions

Coaxial connectors 4.3-10

The new 4.3-10 interface is based on unique radial contact design, offers very low PIM and excellent return loss independent of applied torque while giving the user freedom to choose his preferred male coupling mechanism (torque, hand screw and quick lock). The 4.3-10 interface also offers protection of contact areas against external damages reducing installation errors and 40 % reduction in size and weight. The interface is ideal for telecommunications applications such as macro cell, DAS, in-building and small cells.

› hubersuhner.com

HUBER+SUHNER AG 9100 Herisau/Switzerland
HUBER+SUHNER INC. Charlotte NC 28273/USA

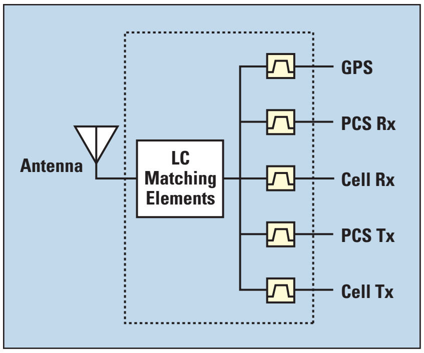

▲ *Fig. 1 Quintuplexer comprising five filters with dissimilar passband frequencies.*

front-end, as well as simplify and accelerate the integration into the phone. Introduced several years ago, multiplexers have become a standard way to optimize, miniaturize and simplify the filtering needs of multi-band phones, requiring only a single antenna to cover multiple bands without a switch between the antenna and the frequency filters.[4] As an example, the functional block diagram of a quintuplexer is shown in ***Figure 1***. Since CA requires different bands to be on at the same time (i.e., no switching between bands), a multiplexer is a convenient implementation to meet CA filtering needs.

Although common in earlier wireless generations, the RF front-end architecture of LTE phones no longer incorporates inter-stage filters between the transceiver and the PA in the transmit path. All FDD frequency filtering is now done by the duplexer or multiplexer, which puts stringent performance requirements on the filters. Any spurious signal from the PA toward the antenna needs to be rejected in the Rx path to not degrade phone sensitivity. This Tx/Rx isolation requirement in the duplexer specification is typically pegged at 55 dB minimum at the Tx and Rx frequencies. The filters inside the CA multiplexer must provide high Tx/Rx isolation, not only within a single FDD band but also across the different FDD LTE bands used in CA.

Driven by size and performance requirements, essentially all RF filtering devices in the handset incorporate surface acoustic wave (SAW) or bulk acoustic wave (BAW) resonator filter technologies. Both SAW and BAW technologies utilize piezoelectric resonators as the basic building block and are well established, mature technologies for RF filtering. For the filter designer, noteworthy SAW or BAW resonator properties are acoustic coupling (kt^2) and Q-factor. Combining resonators to create a filter, ***Figure 2a*** illustrates a 1-stage half-ladder filter topology, a basic element for many filters. This configuration forms a passband when the series resonator has a higher resonance frequency than the shunt resonator (see ***Figure 2b***). Based on this basic topology, any practical filter cascades multiple half-ladder stages to provide sufficient degrees of freedom to meet any realistic in-band and out-of-band filtering requirements. By doing so, the multi-stage filter arranges its poles within the passband, and the zeros outside its passband.

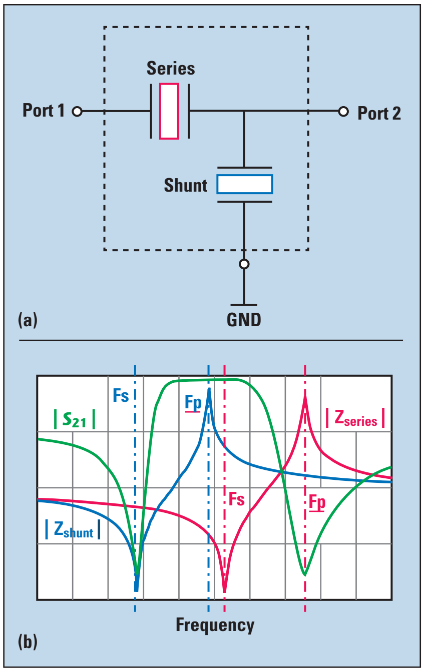

▲ *Fig. 2 One stage half-ladder filter topology (a) with corresponding resonator impedances (Zseries, Zshunt) and filter response (b). Practical implementations of this basic filter topology use multiple stages.*

Combining two filters into a duplexer is the simplest form of a multiplexer. When combining RF filters into a CA-compatible multiplexer, there are two essential design constraints. First, all filters in the multiplexer must be matched at the common antenna node. For any of the passband frequencies, only the respective filter is terminated at the antenna port's impedance Z_{ant}, to minimize RF reflections between the antenna and the multiplexer in the phone; all other filters must appear as open circuits, such that there is no signal leakage into any other filter path. Secondly, high Tx/Rx isolation, both in band and cross-band, is needed for CA use of the multiplexer.

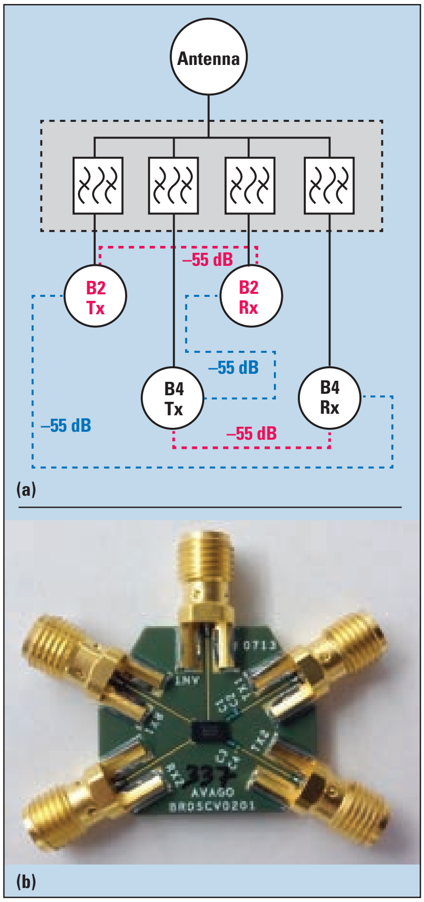

▲ *Fig. 3 Band 2/4 quadplexer block diagram (a) and evaluation board (b). The dotted lines show high Tx/Rx isolation paths needed for carrier aggregation.*

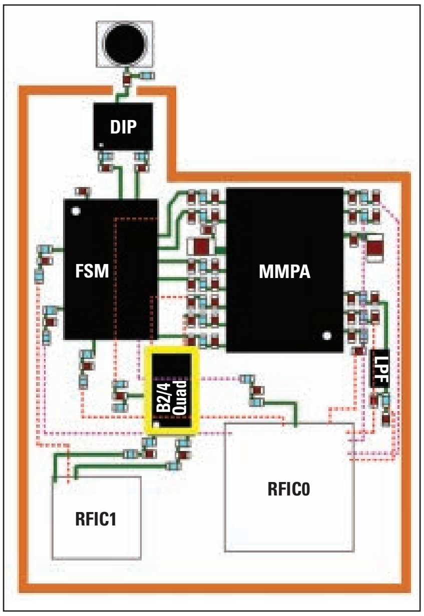

▲ *Fig. 4 Band 2/4 quadplexer on the PCB of the RF front-end module.*

TABLE 1

BAND 2/4 QUADPLEXER PERFORMANCE

(dB)	Tx Insertion Loss	Rx Insertion Loss	Tx Band Isolation	Rx Band Isolation	Tx $2f_0$ Rejection	Tx $3f_0$ Rejection
Band 2	2.0	2.9	58	59	37	38
Band 4	2.0	2.0	61	60	41	14

TABLE 2

BAND 2/4 QUADPLEXER CROSS-BAND ISOLATION

(dB)	Tx Band Isolation	Rx Band Isolation
Band 2 Tx to Band 4 Rx	60 (B2)	65 (B4)
Band 4 Tx to Band 2 Rx	62 (B4)	61 (B2)

In the engineering of the multiplexer module, parasitic crosstalk or direct Tx/Rx signal leakage can degrade isolation and will need to be evaluated in the finished product. Both items need to be addressed in the CA-compliant multiplexer product design. Techniques to address these constraints are well understood.[5,6] Finally, the filter designer uses circuit simulator software as well as 3D electromagnetic simulation to predict multiplexer performance.

BAND 2/4 QUADPLEXER

CA is being deployed in many locations around the globe and CA-capable multiplexers of corresponding LTE band combinations are emerging in the market. For the American wireless market, a recent implementation of a CA-compatible multiplexer is the Band 2 (1.9 GHz PCS) / Band 4 (1.7/2.1 GHz AWS) quadplexer (see ***Figure 3***). Bands 2 and 4 are common North American FDD bands, and since carrier aggregation is already available in some locations,[7] there is a tangible product need for such a quadplexer module. CA-compatibility underscores the value proposition of the Band 2/4 quadplexer module; however, the engineering is challenging for multiple reasons:

Band 2 Duplexer: The filter band gap (Tx/Rx) is relatively narrow, approximately 1 percent of the operating frequency between 1910 and 1930 MHz. Low insertion loss at both filter passband corners (Band 2 Tx high channel and Rx low channel) requires a sharp roll-off for both Tx and Rx filters. This is non-trivial, even without other filters multiplexed to the same antenna node.

Band 4 Duplexer: The filter passbands with low insertion loss are relatively easy to achieve, since the passband width is narrow and the Tx/Rx band gap is large. However, maintaining high Tx/Rx isolation over this large frequency gap can challenge manufacturing tolerances, since most of the signal suppression is purely electrical (L-C resonance, far from the acoustic zeros of the other filter).

CA-Compliance: High cross-band isolations are additional requirements on the filters (B4 Tx/B2 Rx, B2 Tx/B4 Rx, given the second multiplexer design constraint noted previously). Additional out-of-band attenuation requirements typically trade off against in-band performance (i.e., insertion loss) and need to be balanced carefully.

The passbands of the Band 2 and Band 4 filters are relatively close in frequency, with the Band 4 filter frequencies bracketing both Band 2 passbands. The antenna match cannot rely on a diplexer circuit to isolate filter bands; all filters in this quadplexer need be co-designed to optimize the antenna match and ensure high Tx/Rx isolation (all in-band and cross-band combinations).

Increasing the number of filters connected to the same antenna node leads to increased insertion loss in each filter passband. This is unavoidable since the open circuit condition is never perfect or lossless (refer to the first multiplexer design constraint noted above). Elaborating on this point: to optimize multiplexer performance, it is not only helpful to reap low loss and high Q resonance performance of the resonator building blocks for good in-band filter performance, it is also helpful to garner low loss resonator performance at off-resonance frequencies. With low loss off-resonance performance, the open filter matching condition at the antenna port can be implemented with minimum parasitic loss and does not drain signal off the

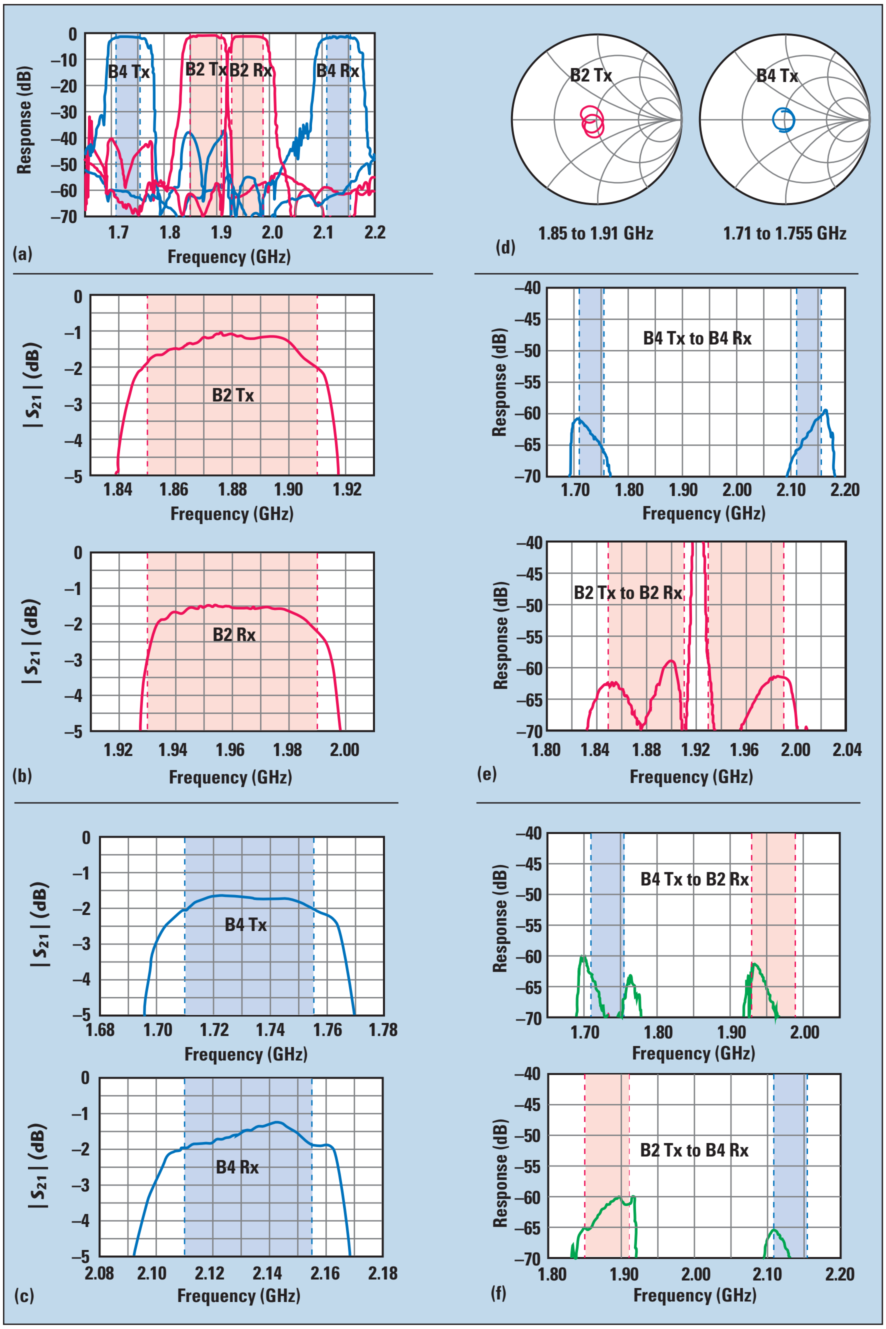

▲ *Fig. 5 Measured performance of a Band 2/4 quadplexer showing the frequency coverage (a) Band 2 insertion loss (b) Band 4 insertion loss (c) Bands 2 and 4 Tx impedance match (d) in-band Tx/Rx isolation (e) and cross-band Tx/Rx isolation (f).*

in-band performance of any passband. Using available SAW or BAW resonator filter technologies, part of the Band 2/4 quadplexer optimization process is minimizing the losses of all four filters at all four passband frequencies.

CA-compatible quadplexers for the Band 2/4 combination have been demonstrated by multiple suppliers, and some are available for sale. ***Figure 4*** shows how the quadplexer would typically be integrated with the other RF components in the front-end of a smartphone. Measured performance of an Avago Band 2/4 quadplexer are shown in ***Figure 5*** and the key performance parameters are summarized in ***Tables 1*** and ***2***. The measured data reflects the recommended circuit matching elements.[8]

This quadplexer uses FBAR technology, a flavor of BAW resonator technology. FBAR is known for low loss resonators, both on and off resonance. Low loss fuels the performance of the quadplexer which, in turn, optimizes the phone's performance and user experience: providing increased sensitivity and battery life, while benefitting from fast wireless data traffic using CA.

CONCLUSION

Smartphones continue to excel in popularity and market penetration, and their computing power and wireless connectivity are steadily improving. LTE-Advanced CA of different LTE bands is being rolled out to increase wireless data rates. As this deployment of band combinations continues across different geographies, corresponding CA multiplexers are emerging in the market. These components optimize RF performance, space and ease of integration for handset OEMs. Low loss filter technologies such as FBAR will continue to enable multiplexer performance. Higher levels of integration are feasible for future CA multiplexers, such as integrating three or more FDD bands. When designing such a multiplexer module, filter losses and antenna match need to be managed carefully to ensure an attractive product. ■

References

1. A. Smith, "U.S. Smartphone Use in 2015," Pew Research Center Internet & Tech, www.pewinternet.org/2015/04/01/us-smartphone-use-in-2015/, April 2015.
2. H. Dediu, "Late Late Majority," www.asymco.com/2014/07/08/late-late-majority/, July 2014.
3. J. Wannstrom, "Carrier Aggregation explained," www.3gpp.org/technologies/keywords-acronyms/101-carrier-aggregation-explained, June 2013.
4. A. Chien, "Multiplexers for Multi-Band Wireless Handset Applications," *Microwave Journal*, Vol. 50, www.microwavejournal.com/articles/print/5095-multiplexers-for-multi-band-wireless-handset-applications, July 2007.
5. A. Link, "Innovative and Proven Approaches for Acoustic Filter, Duplexer and Multiplexer Design," *IEEE-IMS*, WFF-3-362, Phoenix, Ariz., May 2015.
6. T. Jamneala, P. Bradley, D. Feld, D. Clark and A. Chien, "A Generic Passive Matching Network for Multiplexers," *IEEE Transactions on Ultrasonics, Ferroelectrics and Frequency Control*, June 2007.
7. "LTE Carrier Aggregation Technology Development and Deployment Worldwide," *4G Americas*, www.4gamericas.org/files/8414/1471/2230/4G_Americas_Carrier_Aggregation_FINALv1_0_3.pdf, Oct. 2014.
8. Avago B2–B4 quadplexer, ACFM-7024; www.avagotech.com/pages/en/rf_microwave/fbar_filters/multiplexers/acfm-7024/.

NI Wireless Test System

National Instruments
Austin, Texas

Earlier this year, Tesla Motors CEO Elon Musk commented that in the future, "people may outlaw driving cars because it's too dangerous." He was referring to autonomous-drive vehicles sharing the road with other human-controlled cars. Several companies are working toward a reality that envisions you sitting back and reading this magazine while your car transports you safely, comfortably and efficiently to your destination. While you are fully engrossed in the magazine article, your connected car is occupied with processing multiple streams of data from multiple sources, including an important rescheduling notice from the office, road traffic signs, highway warning systems and other vehicles in the vicinity.

Several key technologies will ultimately make this vision of the Internet of Things (IoT) or Internet of "Everything" possible. For instance, once it's defined, next generation wireless infrastructure, or 5G, will provide a wider data pipe for a larger number of users, based on technologies like massive MIMO, higher frequency bands and new waveforms. Another enabling technology is the creation of more tightly integrated chips, modules and devices that combine wireless connectivity with greater processing power. These devices must support an expanding number of complex wireless standards on a growing collection of radio bands.

Having this kind of wireless connectivity in every device with which people interact forces the cost model of these devices to change. Although consumers have the expectation that devices purposely built for wireless networking – such as cellular phones, access points, and home monitoring systems – have a high price premium for this functionality, for other "things" that now connect to the Internet, consumers might not want to bear the extra cost. Although semiconductor system integration reduces the cost of component production, wireless devices manufacturers still have the costly burden of testing each one rapidly and reliably.

NI'S NEW WIRELESS TEST SYSTEM

NI recently released a new Wireless Test System (WTS) to address the need for a cost-effective test solution that can keep pace with evolving wireless technologies. Based on the PXI platform, the WTS uses a high bandwidth PXI chassis, a quad-core Intel i7 embedded PC and one or more of the award-winning NI

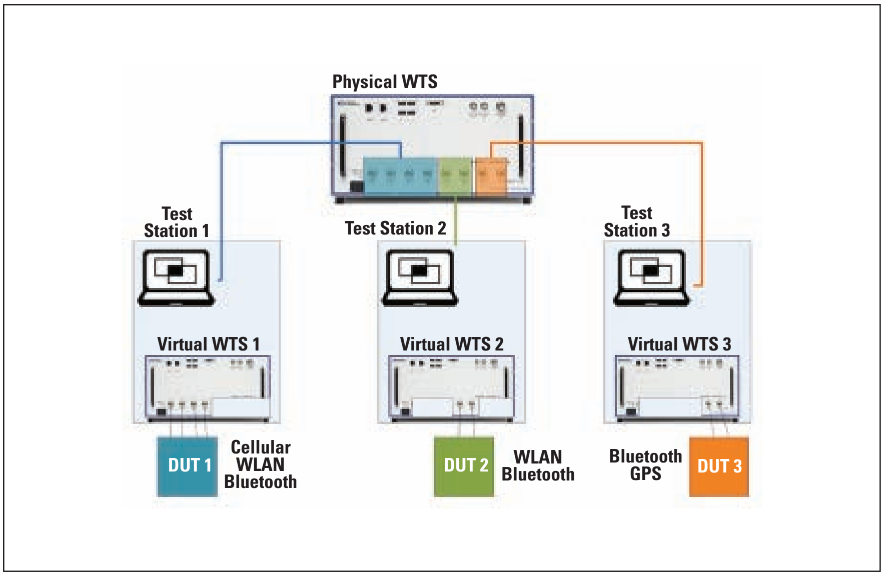

▲ *Fig. 1 Expanding the WTS into multiple virtualized instruments.*

vector signal transceivers (VST). This PXI configuration is internally connected to a rugged RF switch with 8 or 16 Type N RF ports. A metal enclosure makes the system robust enough to meet the demands of high volume production environments.

One of the unique features of the WTS is that you can remotely control it from a PC through a LAN bus using standard commands for programmable instruments (SCPI). With this architecture, the instrument uses a SCPI interpreter to decipher commands and apply the appropriate measurement software. WTS supports measurements for both cellular (from GSM to LTE-A) and wireless connectivity devices (WLAN and Bluetooth). The software algorithms for these measurements are identical to those of other PXI RF test configurations.

REDUCING TEST COST

In addition to the need for modern test systems to reduce capital expenditures, test engineers are required to maximize test throughput – often measured in number of devices tested per hour – and implement parallel test architectures and techniques, while simplifying test development efforts. Typically, test of wireless networking devices requires inserting and removing the device under test (DUT), booting up, configuring the DUT for every test step and performing measurements with the test instruments. In practice, the test system utilizes the RF instruments for only a fraction of the time when testing one device at a time. Given the complexity of wireless test plans for today's devices, testing just one device is an inefficient use of the instruments. As a result, parallel test using a multi-port RF instrument is a common approach that can reduce measurement dead time by making sure that a given test site can access the RF instrument while the other sites are busy with non-measurement tasks. Although the idea of parallel test is simple in theory, implementing a parallel test approach greatly increases the complexity of the test solution.

For example, parallel test requires developers to write test sequences to control and intelligently synchronize both the instrument and the DUTs. Typical test sequences must be designed for multiple sites, keeping track of multiple instrument handles, signal routes and system variables. As a result, designing test software to implement parallel test is a daunting challenge.

Although solving this challenge is difficult with traditional tools, the new WTS simplifies the process with several advanced software features. Two key features of the WTS that simplify parallel test development and make it more scalable are instrument virtualization and pre-coded test steps. Instrument virtualization allows a single WTS to appear – and be programmed as – multiple separate and independent instruments. Using this feature, test developers can write test sequences for a single DUT with their independent, virtualized instrument in mind (see ***Figure 1***). A second key feature is the use of preconfigured test steps with integrated DUT control. These test steps are part of the new NI TestStand Wireless Test Module, an extension of TestStand, the industry-standard test management software. Using the Wireless Test Module, a developer can drag, drop and configure test steps to build a sequence for a single DUT (single site). When the Wireless Test Module executes the sequence, it automatically maps the WTS' RF ports to multiple parallel and independent test sockets, each of which talks with its own virtualized WTS for multi-up DUT testing.

Implementing these techniques has already benefited the testing of intricate automotive infotainment modules that come equipped with multi-band, multi-standard cellular, WLAN and Bluetooth radios as well as GPS receivers, many from different device manufacturers. According to Harman International Industries, this novel approach to test their multi-radio infotainment modules with NI's WTS allowed them to realize important test time reductions.

The WTS' powerful PXI hardware platform in combination with its SCPI interface and intelligent software for implementing the latest cost-saving test architectures give manufacturers of wireless devices the flexibility to keep pace with the advances of the wireless test industry. Even more exciting, once 5G is defined, the combination of NI's WTS instrument virtualization and the Wireless Test Module for test parallelization will enable test engineers to boost test throughput and ultimately lower the cost of testing mobile communications products and the wireless devices that will power the industrial and consumer Internet of Things. With this advance, we can look forward to a world where producing connected cars, homes and a variety of smart appliances is economically viable.

VENDORVIEW

National Instruments
Austin, Texas
www.ni.com

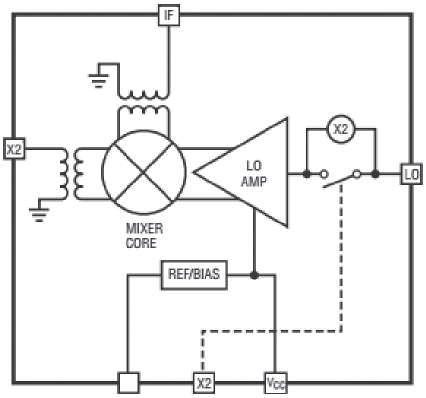

Broadband, High IIP3 Mixer Moves More Data

Linear Technology Corp.
Milpitas, Calif.

To cope with ever increasing Internet traffic, the bandwidth of next-generation wireless access is rapidly expanding. At the same time, the current spectrum simply cannot support the needed bandwidth, so higher frequencies are being evaluated. Multiple options from unlicensed 5.8 GHz terrestrial stations to fleets of low-orbit satellites blanketing the Earth, are being considered. The path to higher bandwidth lies with higher frequencies to deliver on that promise, requiring new mixers with improved performance. The new LTC5549 mixer from Linear Technology has been launched to support just this need.

The LTC5549 is a passive double balanced mixer that functions as either an up- or down-converter. It has a very wide RF frequency range from 2 to 14 GHz. The mixer offers exceptionally high linearity – 28.2 dBm IIP3 at 5.8 GHz and 22.8 dBm at 12 GHz – that improves the dynamic range of both transmitters and receivers. The LTC5549 enables efficient microwave transmitter and receiver designs with an integrated LO buffer that needs only 0 dBm drive, effectively eliminating the need for external high power LO drivers. The LTC5549 also has an integrated, bypassable frequency doubler for the LO signal, allowing the device to use lower cost, commonly available low frequency synthesizers. The double balanced mixer employs wideband integrated balun transformers, optimized to extend the LO and RF frequency bandwidth while enabling single-ended operation. Its IF supports a wide bandwidth from 0.5 to 6 GHz. All three ports are matched to 50 ohms and have excellent port-to-port isolation, minimizing undesirable LO leakage, which eases external filtering.

SiGe BiCMOS TECHNOLOGY

Most microwave mixers are built using discrete GaAs diodes or FETs in hybrid modules. In contrast, the LTC5549 is constructed using a very high frequency advanced SiGe BiCMOS process. SiGe BiCMOS enables a high level of integration, including the on-chip LO buffer and microwave balun transformers. The monolithic die is flipped and soldered onto a tiny 3 × 2 mm lead-frame and encapsulated in a plastic surface-mount package. Bond wires and their associated inductance are eliminated to enhance the device's microwave performance. The inherently small package, along with minimum external circuitry, makes for a very small footprint.

The new mixer's 22.8 dBm IIP3 is a standout in its class and enhances the dynamic range of receivers or transmitters. For a receiver, the higher IIP3 boosts robustness in the presence of close-in high power interference, whether from out-of-band, unintentional emitters or self-induced, such as leak-through from another transmitter in multi-sectored systems. Higher dynamic range receivers provide added design margin and are more forgiving in handling high blockers – as airwaves continually degrade with additional radio deployments.

Similarly for transmitters, a higher IIP3 (hence higher OIP3) mixer produces lower spurious products and improves spectral purity with better ACPR performance. This is particularly important for radios that use higher order modulation, such as 1024 QAM. The improved linearity produces better definition and accuracy of the constellation. Additionally, higher IIP3 allows the mixer to operate at elevated input power and, therefore, more robust output power. The extra design margin eases design constraints, providing flexibility.

DESIGN DIFFERENTIATION

The LTC5549's integrated LO amplifier effectively eliminates the +10 to +17 dBm LO amplifier that is typically required to drive traditional passive microwave mixers. Its 0 dBm LO input level enables the mixer to be driven directly from a PLL/synthesizer without a buffer amplifier. As well as reducing cost, the low LO power produces significantly lower LO leakage to the IF and RF ports, so less external filtering is necessary to contain any out-of-

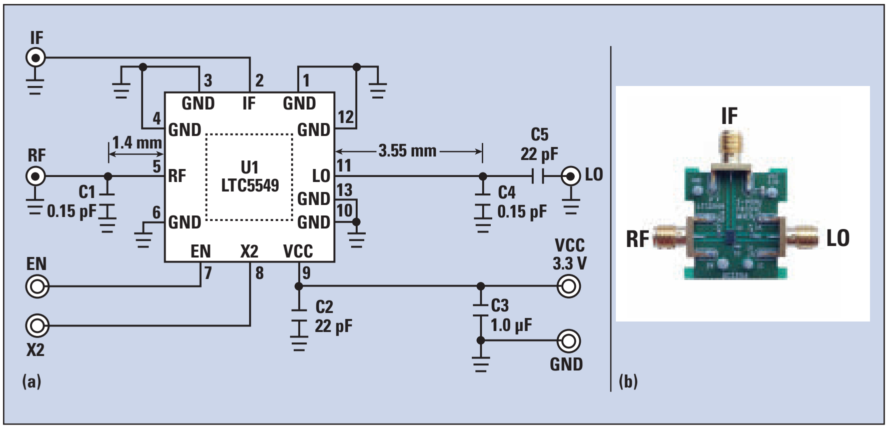

▲ *Fig. 1 LTC5549 evaluation board schematic (a) and assembly (b).*

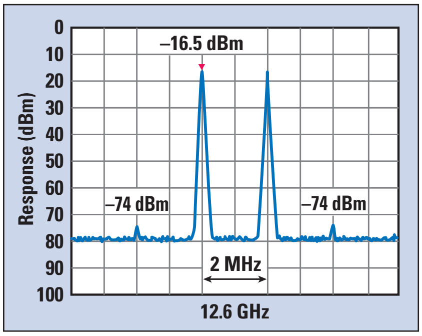

▲ *Fig. 2 Third-order intermodulation measurement at 12.6 GHz with 2 MHz tone separation.*

band emissions associated with the source. Another benefit is not having a high power radiation source on the PC board. This also lowers cost by reducing the RF shielding that plagues many designs requiring high power LO signals.

The LTC5549 incorporates patent-pending advances in planar balun transformer designs, enabling the monolithic mixer to operate over an extremely wide bandwidth. Unprecedented symmetry is achieved, with exceptional balanced operation, optimum spurious cancellation and flat frequency response. For example, the 50 ohm RF port with its built-in transformer and a 0.15 pF external capacitor achieve better than 10 dB return loss from 2 to 14 GHz. Similarly, with a 0.15 pF shunt capacitor and a series capacitor at the LO input, the port is matched from 1 to 12 GHz; return loss better than 10 dB across that entire frequency range. 5G is expected to deliver 1 Gbps data rates. To achieve such speeds, instantaneous radio bandwidth will need to be 1 GHz or higher. The LTC5549 has excellent bandwidth that can support a flat response of more than 1 GHz.

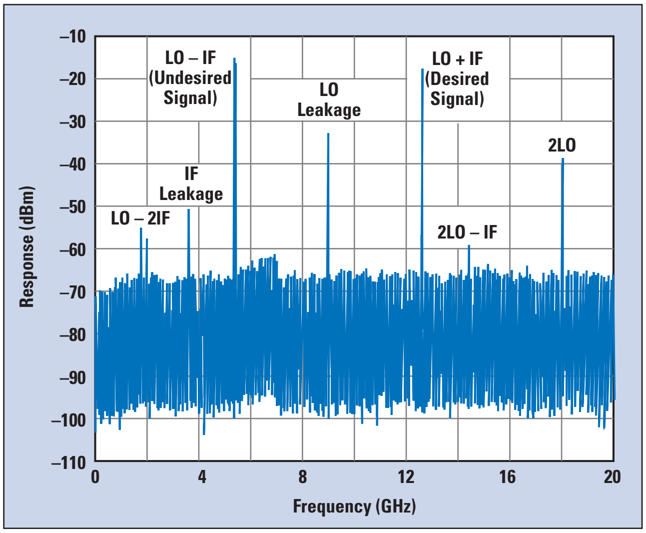

▲ *Fig. 3 Wideband output spectrum showing all spurious products.*

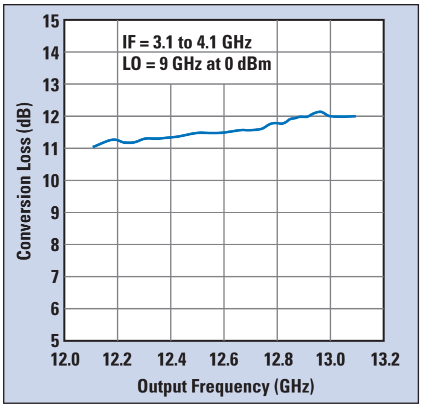

▲ *Fig. 4 The up-conversion mixer conversion loss is approximately 11.5 dB at 12.6 GHz with 1 dB flatness over a 1 GHz bandwidth.*

Microwave test equipment also benefits from a compact, high linearity mixer such as the LTC5549. As RF test equipment pushes to higher frequencies, linearity and bandwidth performance must also be improved to keep pace with the performance of the device-under-test.

3.6 TO 12.6 GHz UP-CONVERTER

To show the performance of the LTC5549, the mixer is used for an up-converter that converts a 3.6 GHz IF signal to a 12.6 GHz RF carrier. The internal 2× LO option is bypassed, so a 0 dBm, 9 GHz signal from a clean laboratory signal source generated the low-side LO drive.

Performance measurements were made using a standard LTC5549 evaluation board (see ***Figure 1***). Because the mixer and evaluation board's components are broadband matched, the board was used as is, without alteration.

Figure 2 shows the mixer's linearity at 12.6 GHz, using two -5 dBm tones separated by 2 MHz. The output third-order intermodulation distortion spurs measured -57.5 dBc, corresponding to an IIP3 of +23.8 dBm. The RF output spectrum from DC to 20 GHz is shown in ***Figure 3***. No external filtering was used to see where all the spurious products fall. The LO leakage power was some 14 dB less than the 12.6 GHz carrier and 3.6 GHz below the carrier frequency, so filtering will not be an issue. The 2LO-IF product is the closest spur and falls 1.8 GHz away from the carrier, with a residual power better than -40 dBc. At 12.6 GHz, the mixer's output exhibited 1 dB flatness over a 1 GHz bandwidth (see ***Figure 4***), showing it is capable of supporting next-generation broadband radios.

The LTC5549 exhibits excellent IIP3 that can enhance the dynamic range of either receiver or transmitter applications. It has an integrated LO buffer, producing very low LO leakage and reducing cost. Its integrated on-chip balun transformers provide extraordinarily wide bandwidth to simplify designs and enable a very compact layout.

VENDORVIEW

Linear Technology Corp.
Milpitas, Calif.
www.linear.com

Smart System Solution for IoT Radio Communications

LoRa™

IMST GmbH
Kamp-Lintfort, Germany

The Internet of Things (IoT) is the recognized next step of ubiquitous networking of machines and devices. Smart appliances currently evolve in conjunction with small, lightweight devices which generate completely new requirements for the underlying radio communication technology. Significantly, material costs of these devices are often well below $10, such that a wireless communication component has strong demands on the target pricing. The classical ISM bands are suitable candidates for license-free radio communications, utilizing cheap radio transceivers compared to WLAN solutions or cellular radio technologies. However, transmission ranges of only a few meters have been a significant hurdle to network implementation in the past.

To address this issue, a new transceiver front-end technology called LoRa™ (an abbreviation for long range) has been developed and patented by the semiconductor company Semtech. It allows for much longer distances compared to the classical ISM band radio front-ends, with up to 15 km range. The long range is achieved under line-of-sight conditions using a correlation mechanism based on spread spectrum technology in the front-end of the transceiver, with the trade-off of reduced transmission bit rates at the longer distances.

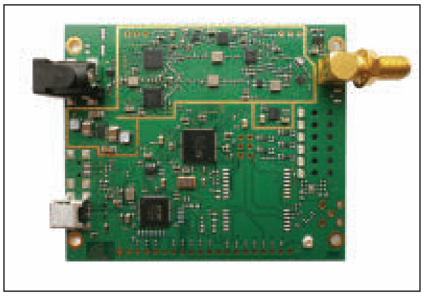

▲ *Fig. 1 The IMST LoRa iC880A concentrator module.*

Cellular systems with a coverage area of many square kilometers are possible. According to the envisaged applications, tens to hundreds of end nodes will have to be handled within one communication cell. Thus, the central communication point – the concentrator, as the radio part of a LoRa gateway – must be capable of massive parallel receive operation on many channels, each of them individually configured for certain distances and bit rates. There are many applications which will be supported by long range cellular license-free communications such as agriculture, industrial, logistics, smart environment, smart metering, smart city and smart home. Public telecom operators as well as private companies are currently implementing LoRa-based system solutions with the corresponding access networks and the necessary IT infrastructure. The deployment of LoRa technology is structured and organized by the LoRa Alliance (www.lora-alliance.org), where semiconductor companies, radio equipment manufacturers, firmware and software providers, mobile operators, IT companies and test houses work together to set up a complete LoRa ecosystem, including the required quality procedures and system certifications.

The novelty of the air interface is mainly characterized by the introduction of a spreading factor, which denotes the relationship of transmission time to bit rate due to the spread spectrum transmission mentioned earlier. It utilizes a bandwidth of 125, 250 or 500 kHz in the available ISM radio bands (e.g., about 868 MHz in Europe), together with frequency selection and frequency hopping options, to transmit with a transmitter-specific hopping code for user separation. A transmission channel is mainly characterized by the spreading factor and the frequency. The configuration parameter space is enhanced by two very important dimensions utilizing these two parameters.

Whereas the end nodes are capable of transmitting data packets on only one channel, the current IMST concentrator module – iC880A – is able to receive packets of different end nodes on eight channels in parallel. The IMST LoRa iC880A concentrator module (see ***Figure 1***) is fully certified according to the European R&TTE guidelines, offering a comprehensive set of firmware options for media access and networking. Operating in the 868 MHz frequency band and measuring 79.8 × 67.3 mm, key features include: sensitivity down to -138 dBm, output power to 20 dBm, USB or SPI interface with optional GPS, SX1301 baseband processor, 2 × SX1257 Tx/Rx front-ends, 49 × LoRa demodulators, 1(G)FSK demodulator and 8+1+1 parallel demodulation paths for LoRa and GFSK demodulation. A complete LoRa explorer kit is available for networking trials, and LoRaWAN™ and IMST LR_Base/LR_Starnet firmware is available for the optimal choice of MAC and networking features.

The concentrator architecture is fully scalable if more channels are required, with the expense of additional hardware. Several users may share a channel in the time domain if a duty cycle for each user is introduced. With this capability of parallel reception, the handling of large LoRa cells with hundreds of end nodes is feasible and maintainable.

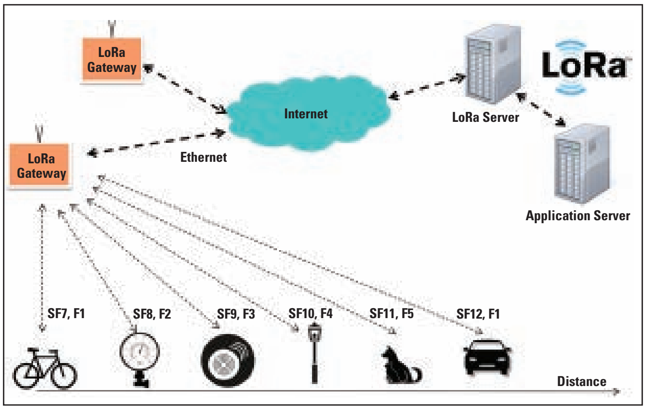

▲ *Fig. 2 Typical architecture of a LoRa network with different applications and different spreading factors (SF) and frequency channels (F). The concentrator is the central radio part of the gateway.*

While a mesh network structure always imposes a heavy protocol overhead, which does not fit with the notion of lightweight implementation, a star structure with a central communication point in the middle of a cell appears to be the right means of administering the deployed end nodes with central control, strong synchronization and minimum protocol overhead (see ***Figure 2***).

The protocol stack firmware has to cope with such new and promising architecture and use cases with their specific user scenarios. Communication capacity has to be optimized – this is particularly important with the lower bit rates compared to traditional short range wireless communication. Furthermore, the media access control (MAC) has to be organized in such a way that the number of collisions on the radio channel is minimized and the transmitted power and used spreading factor are set to the actual required minimum, depending on the data rate and the distance of the end nodes to the concentrator in the middle of the cell.

This is done with an adaptive data rate (ADR) access scheme. The first MAC implementations were quite simple with only random access to the channel; since then, more complex MAC designs have been realized. With a view to regulatory requirements, adaptive frequency agility (AFA) and listen before talk (LBT) are two strategies to avoid the duty cycle restrictions of the ISM bands. Other implementations with central control and central synchronization aim to maximize system capacity while minimizing power consumption of the sensors, simultaneously allowing for long term battery operation of the end nodes.

LoRa-based communication systems will complement the mobile networks in an ideal manner – no costs for air time will occur, the devices are inexpensive and can reach long ranges. Gateways built from the concentrator will enable a communication path to the Internet, either via mobile cellular technology, DSL subscriber line, Ethernet or wireless LAN connections.

IMST GmbH
Kamp-Lintfort, Germany
www.wireless-solutions.de
www.webshop.imst.de

Tech Brief

Low g-Sensitivity, Ultra-Low Power OCXOs

CTS Corp.
Elkhart, Ind.

CTS has expanded its OCXO portfolio with the addition of a low g-sensitivity option on their miniature, high performance, ultra-low power OCXOs. Models 144, VFOV405 and VFOV504 now include low g-sensitivity at 10 and 100 MHz to 2^{-10}/g. This is an order-of-magnitude improvement under dynamic conditions. Added to the size, weight, power (SWaP) and other performance features, these products are highly attractive compared to the industry's standard OCXOs, which are large and power hungry.

The 144, VFOV405 and VFOV504 models cover HF, VHF and UHF bands and come in TO-8, cold-welded, evacuated enclosures. The addition of the low g-sensitivity option provides compelling solutions for the most challenging, high performance, frequency control needs, especially under dynamic conditions.

CTS LPOCXOs are designed into defense, aerospace, industrial and commercial applications. They are used in Tx/Rx, GPS and local and master reference sources for ground, airborne, shipboard, undersea and space systems. CTS products are known for precision (≤ 10 ppb, -40°/+85°C), low static phase noise (to -100 dBc/Hz at 1 Hz, -170 dBc/Hz floor) and ultra-low power consumption (to 0.12 W steady state and 0.4 W start-up, typical). This performance is now combined with low g-sensitivity in a TO-8 package. In addition to low g-sensitivity, CTS also addresses the vibration and shock levels associated with all the markets they serve.

CTS Corp.,
www.ctscorp.com,
Albert.Riso@ctscorp.com

Company Showcase

Website Redesign

Anokiwave launched the redesign of their website to provide visitors, customers and partners with relevant and easy-to-find information about their new mmWave Silicon ICs, AESA ASICs and III/V products. The new look and improved functionality allows users to access new product information and the company's blog with articles authored by their engineering team. The new website also includes new product information with datasheets, company overview and leadership team bios, links to Anokiwave's social media pages and the latest company buzz.

Anokiwave Inc.

www.anokiwave.com

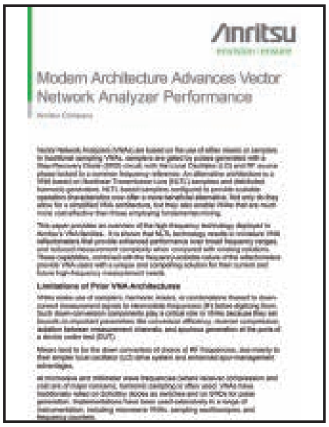

Modern Vector Network Analyzer

VENDORVIEW

Modern Vector Network Analyzer (VNA) architectures such as those based on Nonlinear Transmission Line (NLTL) samplers and distributed harmonic generators now offer a beneficial alternative to traditional sampling VNAs. They allow for a simplified architecture and also enable VNAs that are much more cost effective. It is shown that NLTL technology results in miniature VNA reflectometers that provide enhanced performance over broad frequency ranges and reduced measurement complexity, providing VNA users a unique and compelling solution for their high-frequency measurement needs.

Anritsu Co.

www.goanritsu.com/VNAFam

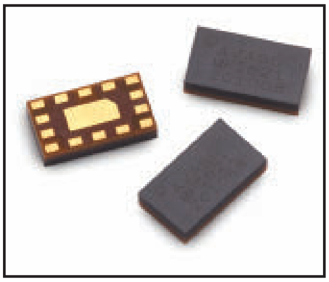

LTE Carrier Aggregation Multiplexers

The number of cellular bands used concurrently under LTE Advanced continues to increase. Multiple carrier frequency bands are being aggregated to provide higher data throughput. Leveraging unique FBAR filtering technology and in-house RF module expertise, Avago Technologies provides the industry's most comprehensive and advanced portfolio of LTE carrier aggregation (CA) multiplexers enabling mobile data aggregation of more than 25 frequency segments.

Avago Technologies

http://go.avagotech.com/LTE-CA

TL-P PIM Test Solutions

VENDORVIEW

The TL-P product line is the ideal solution for bench top PIM analyzers in an indoor environment (lab or factory testing) offering excellent return loss performance. It joins a user-friendly handling that is new to the market, as well as durability and reliable PIM results in one product – an investment that boosts total cost of ownership. With its light weight and smooth physical characteristics, HUBER+SUHNER's TL-P is also a great asset for field test applications.

HUBER+SUHNER

www.hubersuhner.com

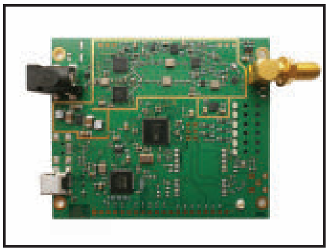

LoRa Concentrator Module

The IMST LoRa™ concentrator module iC880A is targeted for a huge variety of IoT applications. It is a multi-channel, high performance transmitter/receiver module designed to receive several LoRa packets simultaneously using different spreading factors on multiple frequency channels. It can easily be integrated into a gateway as a complete RF front-end. The module is fully certified according to the European R&TTE guidelines. A comprehensive set of firmware options for medium access and networking is available.

IMST GmbH

www.imst.com

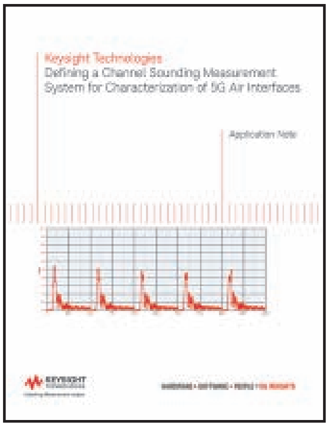

5G Channel Sounding

VENDORVIEW

This new 5G application note provides insight into defining a channel-sounding measurement system for characterization of 5G air interfaces through a variety of measurement methods. The emerging 5G standard will almost certainly incorporate a combination of millimeter wave (mmWave) frequencies, ultra-broad bandwidths and massive multiple-input-multiple-output (MIMO) methods. Although each of these adds difficulty to the design of transmitters and receivers, the most significant unknowns are in the over-the-air radio channels between user equipment and base station. Keysight's 5G solutions are ready to enable deeper insights as the standards evolve.

Keysight Technologies

www.keysight.com/find/5G

Company Showcase

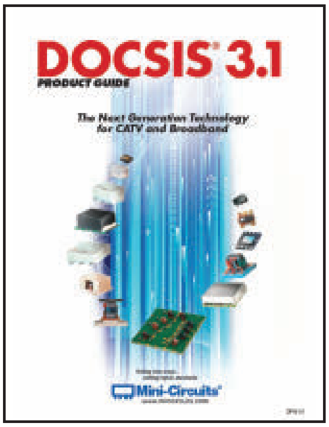

DOCSIS 3.1 Product Guide

VENDORVIEW

Mini-Circuits' new DOCSIS® 3.1 Product Guide, a 116-page full-color catalog, showcases the company's line of "next generation" products for CATV and broadband markets. The guide provides detailed information on Mini-Circuits' wide range of RF components, all carefully specified to meet DOCSIS 3.1 standards. This includes everything from passive devices such as its transformers, couplers, and splitter/combiners to active elements such as amplifiers, equalizers and more. With over 70 different DOCSIS®-compliant models, chances are Mini-Circuits has your application covered.

Mini-Circuits

www.minicircuits.com

NI AWR Design Environment

NI AWR Design Environment V12.01

VENDORVIEW

NI AWR Design Environment™ is complete high-frequency design software for system simulation, circuit simulation, and electromagnetic analysis. V12.01 has been released and continues to build upon the new load-pull features of V12. In addition, the V12.01 update includes multiple improvements to system simulation within Visual System Simulator™, layout, tuning, yield analysis and optimization capabilities within NI AWR Design Environment, inclusive of Microwave Office and AXIEM and Analyst™ 3D EM simulators.

National Instruments

www.ni.com

Channel Sounding Test Solution

VENDORVIEW

Rohde & Schwarz supports research activities to make the spectrum in the millimeter wave range usable for 5G with a new channel sounding solution. It is based on the R&S SMW200A vector signal generator and the R&S FSW85 signal and spectrum analyzer, the only device on the market that covers 2 Hz to 85 GHz in a single sweep without the need of external harmonic mixers. Equipped with the R&S FSW B2000 option, it can even analyze signals with a bandwidth of up to 2 GHz.

Rohde & Schwarz GmbH & Co. KG

www.rohde-schwarz.com

Low PIM Switch for T&M

VENDORVIEW

The saving potential of SPINNER's low PIM switches in RF testing environments is immense. They spare you the hassle of undocking and re-docking measurement cables when performing different measurements on the same DUT. Technically speaking, these are DPDT switches with two parallel-switching inputs and outputs. They are available with 7-16 and 4.3-10 connectors and specified for -165 dBc (typ. -170 dBc). A perfect fit for measuring VSWR and PIM in the frequency range between 330 MHz and 3800 MHz.

Spinner GmbH

www.spinner-group.com

ADVERTISING INDEX & SALES REPRESENTATIVES

ADVERTISER	PAGE NO.
Anokiwave	7
Anritsu Company	9
Avago Technologies	17
CTS Electronic Components	21
Huber + Suhner AG	27
IMST GmbH	25
Keysight Technologies	COV 4
Mini-Circuits	15, 41
Narda Safety Test Solutions GmbH	29
National Instruments (formerly AWR)	11
Pico Technology	19
Pivotone Communication Technologies, Inc.	35
Rogers Corporation	31
Rohde & Schwarz GmbH	COV 3
Skyworks Solutions, Inc.	COV 2
Spinner GmbH	37

Ed Kiessling, Traffic Manager/Inside Sales
685 Canton Street Norwood, MA 02062
Tel: (781) 619-1963 FAX: (781) 769-6178
ekiessling@mwjournal.com

Eastern and Central Time Zones
Chuck Boyd
Northeast Reg. Sales Mgr.
(New England, New York, Eastern Canada)
685 Canton Street
Norwood, MA 02062
Tel: (781) 619-1942
FAX: (781) 769-5037
cboyd@mwjournal.com

Michael Hallman
Eastern Reg. Sales Mgr.
(NJ, Mid-Atlantic, Southeast, Midwest, TX)
4 Valley View Court
Middletown, MD 21769
Tel: (301) 371-8830
FAX: (301) 371-8832
mhallman@mwjournal.com

Pacific and Mountain Time Zones
Brian Landy
Western Reg. Sales Mgr.
(CA, AZ, OR, WA, ID, NV, UT, NM, CO, WY, MT, ND, SD, NE & Western Canada)
144 Segre Place
Santa Cruz, CA 95060
Tel: (831) 426-4143
FAX: (831) 515-5444
blandy@mwjournal.com

International Sales
Richard Vaughan
International Sales Manager
16 Sussex Street
London SW1V 4RW, England
Tel: +44 207 596 8742
FAX: +44 207 596 8749
rvaughan@horizonhouse.co.uk

Germany, Austria, and Switzerland (German-speaking)
WMS.Werbe- und Media Service
Brigitte Beranek
Gerhart-Hauptmann-Street 33,
D-72574 Bad Urach
Germany
Tel: +49 7125 407 31 18
FAX: +49 7125 407 31 08
bberanek@horizonhouse.com

Korea
Young-Seoh Chinn
JES Media International
2nd Floor, ANA Bldg.
257-1, Myungil-Dong
Kangdong-Gu
Seoul, 134-070 Korea
Tel: +82 2 481-3411
FAX: +82 2 481-3414
yschinn@horizonhouse.com

China
Shenzhen
Michael Tsui
ACT International
Tel: 86-755-25988571
FAX: 86-10-58607751
michaelt@actintl.com.hk

Shanghai
Linda Li
ACT International
Tel: 86-21-62511200
lindal@actintl.com.hk

Beijing
Oasis Guo
ACT International
Tel: 86-13011108861
oasisg@actintl.com.hk

Hong Kong, Taiwan, Singapore
Mark Mak
ACT International
Tel: 852-28386298
markm@actintl.com.hk

Japan
Katsuhiro Ishii
Ace Media Service Inc.
12-6, 4-Chome,
Nishiiko, Adachi-Ku
Tokyo 121-0824, Japan
Tel: +81 3 5691 3335
FAX: +81 3 5691 3336
amskatsu@dream.com